AD NUMBER: AD0878331

LIMITATION CHANGES

TO:

Approved for public release; distribution is unlimited.

FROM:

Distribution authorized to US Government Agencies only; Export Control; 28 Feb 1970. Other requests shall be referred to Air Force Materials Laboratory, Wright-Patterson AFB, OH 45433.

AUTHORITY

AFML LTR, 8 May 1974

AFML-TR-70-172

RESEARCH TO DETERMINE THE EFFECTS OF SURFACE CATALYCITY ON MATERIALS BEHAVIOR IN DISSOCIATED GAS STREAMS-ATJ-GRAPHITE

J. B. Berkowitz-Mattuck

ARTHUR D. LITTLE, INCORPORATED
CAMBRIDGE, MASSACHUSETTS 02140

TECHNICAL REPORT AFML-TR-70-172

February 28, 1970

NOTICES

When Government drawings, specifications, or other data are used for any purpose other than in connection with a definitely related Government procurement operation, the United States Government thereby incurs no responsibility nor any obligation whatsoever; and the fact that the Government may have formulated, furnished, or in any way supplied the said drawings, specifications, or other data is not to be regarded by implication or otherwise as in any manner licensing the holder or any other person or corporation, or conveying any rights or permission to manufacture, use, or sell any patented invention that may in any way be related thereto.

Copies of this report should not be returned unless return is required by security considerations, contractual obligations, or notice on a specific document.

RESEARCH TO DETERMINE THE EFFECTS OF SURFACE CATALYCITY ON MATERIALS BEHAVIOR IN DISSOCIATED GAS STREAMS-ATJ-GRAPHITE

J. B. Berkowitz-Mattuck

ARTHUR D. LITTLE, INCORPORATED
CAMBRIDGE, MASSACHUSETTS 02140

FOREWORD

This report was prepared by Arthur D. Little, Inc., Cambridge, Massachusetts 02140, under USAF Contract F33615-69-C-1079. This contract was initiated under Project No. 7360, "Chemical, Physical, and Thermodynamic Properties of Aircraft, Missile, and Spacecraft Materials," Task 736001, "Thermal and Chemical Behavior of Advanced Weapon System Materials." The work was administered under the direction of the Air Force Materials Laboratory, Air Force Systems Command, Wright-Patterson Air Force Base, Ohio 45433, with Paul W. Dimiduk (AFML/LPT) acting as Project Engineer.

This covers work conducted from 15 October 1968 to 31 January 1970 at Arthur D. Little, Inc., with Dr. J. B. Berkowitz-Mattuck as Project Engineer. Contributing personnel were M. Rossetti, C. Lukas, M. Bonislawski, J. Hamlet, J. Aronson, and A. Emslie. Dr. M. Kaufman of the University of Pittsburgh and Dr. D. E. Rosner of Yale University were consultants to the program.

The guidance and assistance of Mr. Paul Dimiduk of the Air Force Materials Laboratory in many phases of this program was of considerable value and is gratefully acknowledged by the author. This manuscript was released by the author, February 1970.

This technical report has been reviewed and is approved.

HYMAN MARCUS, Chief
Thermo & Chemical Physics Branch
Materials Physics Division
Air Force Materials Laboratory

ABSTRACT

The reactions of partially dissociated oxygen with heated ATJ graphite surfaces have been investigated at temperatures of 1600-2800°K and oxygen atom partial pressures of 7.0×10^{-3} to 7.4×10^{-2} torr. Measurements of total oxygen atom decay as a result of both chemical reaction and catalytic recombination were carried out by the $NO-NO_2$ light intensity method in a fast flow system. Weight change measurements were made to separate the total atom loss results into its two components. Mass spectrometric experiments were carried out over the temperature range 400-1200°K to determine product distribution as a function of oxygen molecule dissociation. The rate of net atom loss was found to be linear with time at a given partial pressure, and approximately first order in pressure. The net atom loss rate shows a maximum in the temperature interval investigated, the maximum shifting to higher temperatures with decreasing oxygen atom pressure. At an oxygen atom pressure of 3×10^{-5} atm, chemical reaction accounts for about 50% of the atom loss at low temperature, more than 60% of the atom loss in the neighborhood of maximum rate, and less than 35% of the atom loss at the highest temperatures investigated.

TABLE OF CONTENTS

LIST OF ILLUSTRATIONS

LIST OF ILLUSTRATIONS (CONTINUED)

LIST OF TABLES

LIST OF SYMBOLS

A, surface area, cm^2

$B^2 = k_v r_o^2/D$

C_L, radius of curvature

γ, recombination coefficient; fraction of atoms colliding with a surface and catalytically recombining

γ_{app}, collision efficiency; fraction of atoms colliding with graphite which are desorbed as CO(g), CO_2(g), or O_2(g)

D, diffusion coefficient of oxygen atoms in a gas mixture, cm^2/sec

$\delta = 4D(1-\gamma/2)/\bar{w}\gamma r_o$

ε, fraction of atoms colliding with the graphite surface which are desorbed as CO(g) or CO_2(g)

G, total oxygen atom loss rate, $moles/cm^2$-sec

I, light intensity

I^+, ion intensity (mass spectrometer signal)

J_1, first order Bessel function

k', proportionality constant (eq. [3])

k_v, rate constant for homogeneous atom recombination, sec^{-1}

l, L, reactor length, cm

M, molecular weight

(O), oxygen atom concentration, moles/cc

p, partial pressure

P, total pressure

ρ, total gas density, g/cc

r, radial distance, cm

$r^* = r/r_o$

r_o, tube radius, cm

LIST OF SYMBOLS (CONTINUED)

R, ratio of light intensity readings

T, absolute temperature, °K

U, average linear flow velocity, cm/sec

v_x, linear flow velocity, cm/sec

V, molar volume

$\bar{w}$, kinetic theory average molecular velocity

W, total mass flow rate, g/sec

ψ, mole fraction of oxygen atoms in a gas mixture

z, linear distance, cm

$z^* = z/r_o$

Z, collision rate, moles/cm^2-sec

Subscripts:

O, oxygen atoms

O_2, oxygen molecules

s, stagnation point

T, temperature

av, average

Top, position of top photometer

Bottom, position of bottom photometer

I. INTRODUCTION

In the forward area of a reentry vehicle (nose and/or leading edges), the free-stream velocity is reduced nearly to zero, and practically all of the aerodynamic kinetic energy is converted to thermal energy behind the shock wave in what is called the "shock layer" (the region between the shock wave and the surface of the vehicle). Translational and rotational gas temperatures increase nearly instantaneously on passing through the shock wave; energy is then transferred to the slower responding modes of vibration and dissociation, and translational temperature drops. If relaxation times for chemical equilibrium are slow, a non-equilibrium atom concentration will persist to the surface of the vehicle. In the case of frozen flow, a useful limiting approximation, the diffusion time for an oxygen atom across the boundary layer will be very short compared to the time required for gas phase recombination within the volume of the boundary layer. Consequently, the number of oxygen atoms reaching the surface of the vehicle will be far in excess of the equilibrium number for a gas at the temperature and ambient pressure of the vehicle surface. The interaction of these atoms with the vehicle surface can contribute significantly to the net heat transfer to the vehicle.

Graphite is a leading contender for advanced reentry vehicle applications. A non-equilibrium concentration of oxygen atoms in the vicinity of a graphite surface may interact with the surface in several ways. The atoms may be catalytically recombined to oxygen molecules, with release of energy to the surface; and they may react directly with the surface to enhance the net rate of surface oxidation or recession, with release of $CO(g)$ and/or $CO_2(g)$ into the boundary layer.

The experimental program discussed below was directed towards a study of the kinetics of heterogeneous recombination and surface oxidation of ATJ graphite under conditions of temperature and pressure that might be extrapolated to typical reentry environments. A threefold approach was pursued involving: (1) use of a fast flow apparatus to measure total atom loss rates when non-equilibrium concentrations of oxygen atoms impinge on an inductively heated graphite surface; (2) measurement of weight changes

on ATJ samples exposed to O/O_2 gas mixtures for various times at temperatures; and (3) mass spectrometric determination of product distribution.

II. FAST FLOW SYSTEM EXPERIMENTS

A fast flow apparatus has been developed to monitor the decay of oxygen atoms due to recombination and chemical reaction with an inductively heated ATJ graphite ring sample. As indicated schematically in Figure 1, oxygen molecules in an argon stream are partially dissociated by means of a 2450 mc/sec generator with a microwave power output of 0-100 watts. Relative atom concentrations along the length of the flow tube are monitored photometrically by introducing a trace amount of NO(g) into the flow gas, upstream of the test section of the apparatus. NO(g) reacts with gaseous oxygen atoms as follows:

$$NO(g) + O(g) \rightarrow NO_2(g) + h\nu \qquad (1)$$

$$NO_2(g) + O(g) \rightarrow NO(g) + O_2(g) \text{ (very fast)} \qquad (2)$$

The very fast reaction (2) assures that the NO(g) concentration remains constant, and hence the intensity of light produced via reaction (1) is directly proportional to oxygen atom concentration. Relative light intensities are usually taken at two points along the flow tube as indicated, although the photometers can be moved for calibration purposes.

The NO(g) concentrations must be maintained within a limited range. If the NO(g) concentration is too small, the light intensities are too weak for accurate measurement. On the other hand, if the NO(g) concentration is too large, an appreciable fraction of the O(g) atoms can be lost via reactions (1) and (2), which complicates the data analysis. A range of NO(g) concentrations was identified experimentally, over which the light intensity ratio remained constant. All measurements were taken in the middle of this range. The NO(g) flow rate was controlled by means of a Pace P-7 Transducer and a Nupro SS-2A valve in series.

One of the major problems encountered in adapting the fast flow system for high temperature measurements has been the very large background radiation in the neighborhood of the photometers from the inductively heated graphite insert. The problem was solved by curving the flow tube

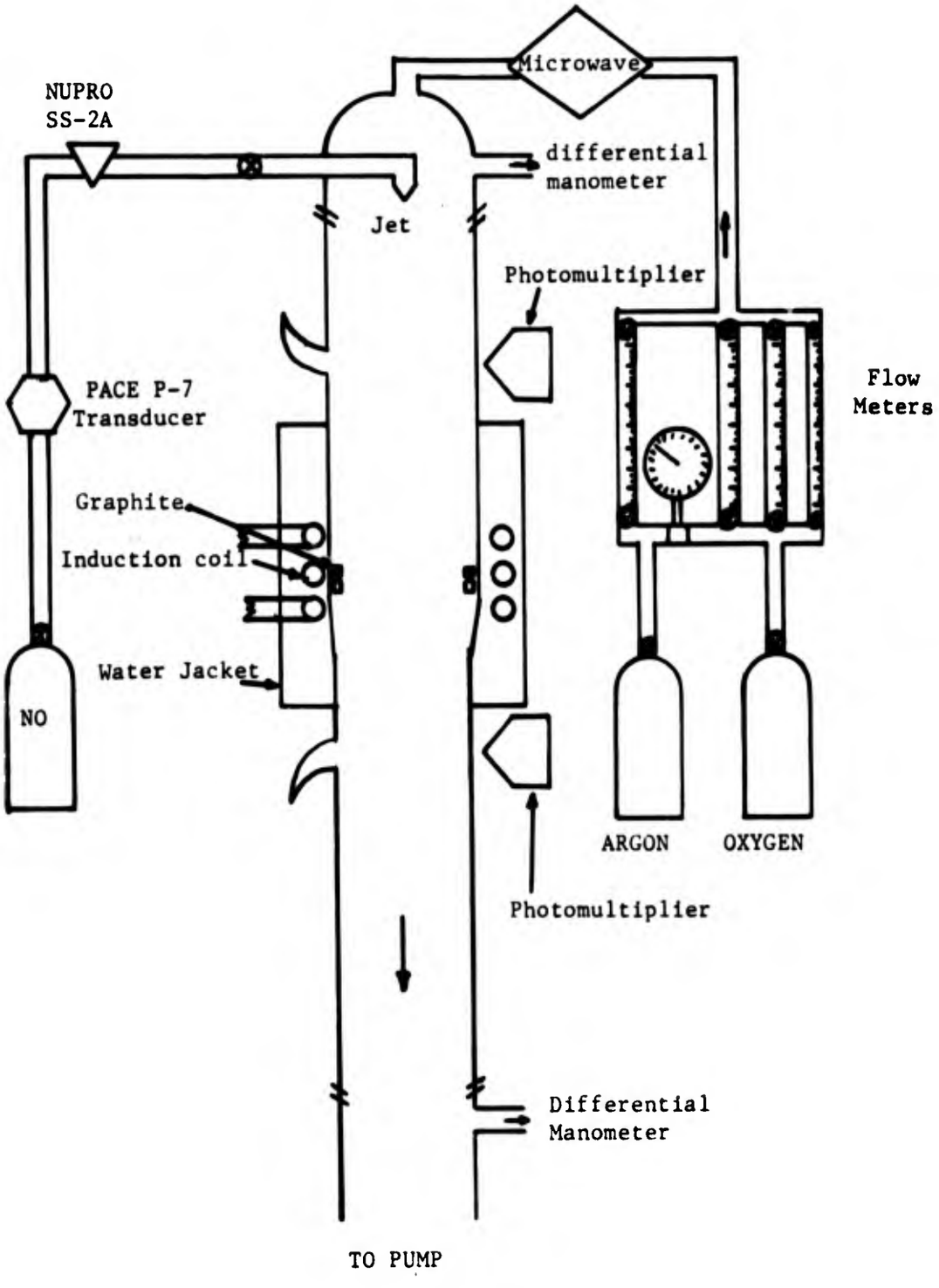

Figure 1. Schematic Diagram of Apparatus for Oxygen Atom Recombination Studies

to eliminate the possibility of direct light paths between the carbon ring and the photometer apertures. The curvature initially introduced was selected solely on the basis of the optical requirements, and the choice proved to be most unfortunate. Results were highly non-reproducible from day to day and even from hour to hour. The problem was ultimately traced to instabilities in the flow system induced by the particular combination of tube curvature and flow parameters selected. After removal of the black optical paint from the outside of the flow tube, the greenish NO afterglow could be observed visually along the length of the tube. The intensity of the glow served as a very sensitive indicator of regions of excessive turbulence, and of changes in flow pattern with very minor changes in such parameters as room temperature, volumetric flow rates, and total pressure.

A number of curved flow tubes were then constructed, and tested for both flow uniformity and signal-to-noise ratio as a function of temperature. Two flow tubes were selected, as drawn schematically in Figures 2 and 3. In both, the NO afterglow intensity observed at room temperature appeared to decrease uniformly from top to bottom of the tube, with no bright spots and no abrupt changes in intensity with small variations in the parameters controlling the flow. The strongly bowed tube of Figure 3 was required for temperatures above 2300°K. Both tubes yielded consistent results at lower temperatures. The introduction of curvature probably does cause eddy currents in the neighborhood of the bends, and increases the effective length of the flow tube over and above the geometric length. However, the uniformity of the NO(g) afterglow suggests that conditions very close to laminar flow were maintained. By comparing the ratio of top and bottom photometer readings, R_T, obtained with the graphite at a temperature T, with a ratio, R_{298}, obtained at room temperature, the difference in rates of atom removal at 298°K and at temperature can be determined. In general, the decrease in oxygen atom concentration along the flow tube between the top and bottom photometers is due to (1) heterogeneous oxygen atom recombination on the quartz walls of the flow tube, (2) homogeneous oxygen atom recombination within the volume of the gas, and (3) hetrogeneous oxygen atom recombination and chemical reaction at the surface of the graphite. Atom loss due to the first two mechanisms is approximately

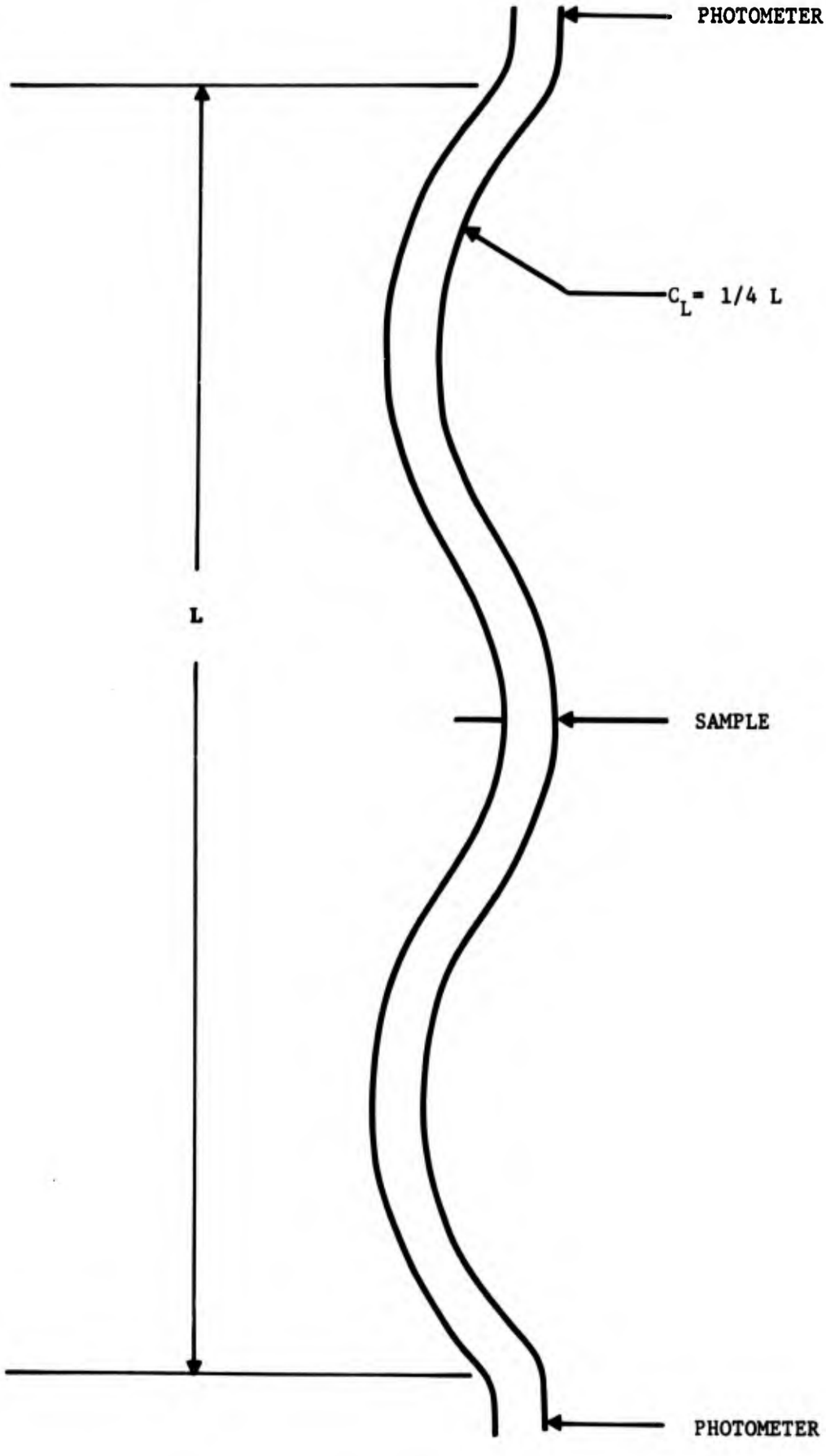

FIGURE 2: TUBE CONFIGURATION USED FOR EXPERIMENTS BELOW 2300°K

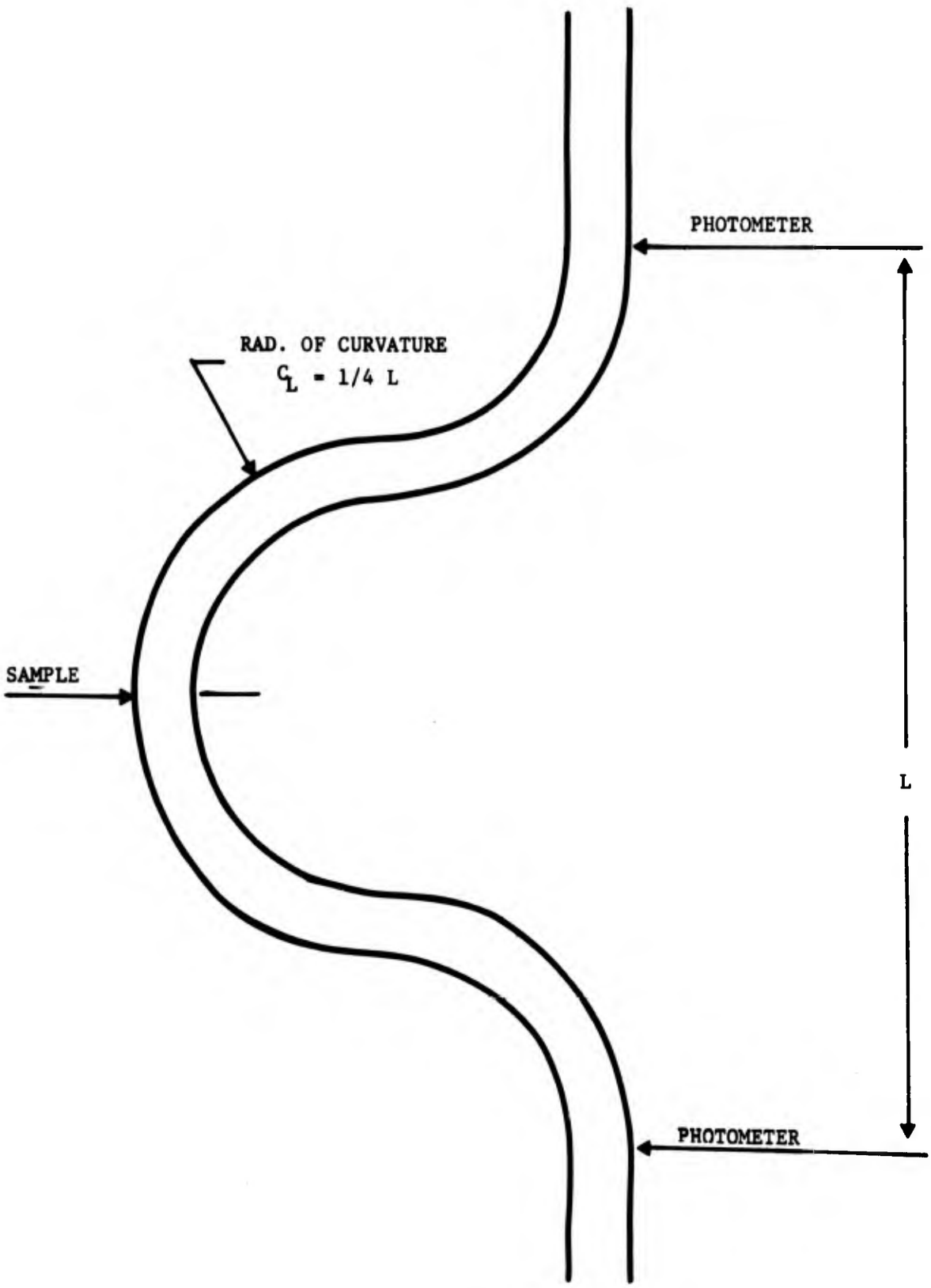

FIGURE 3: TUBE CONFIGURATION FOR EXPERIMENTS ABOVE 2300°K

independent of the temperature of the graphite, since the quartz walls are continuously cooled by means of a water jacket. If all of the reactions are written in terms of first order rate constants[1], R_T/R_{298} reflects the extent of the third reaction only at the two temperatures. With the graphite at temperatures of 298°K and 1200°K, the total distance between the two photometers was varied between 20 and 60 cm (geometric distance), by changing the positions of both the top and bottom photometers. The ratio of R_{1200}/R_{298} remained constant at 1.74 ± 0.07, and showed no trend with the distance of separation or photometer position. The check was made at a relatively low temperature to minimize corrections for background radiation from the heated graphite.

Much of the data in the literature on the rate of high temperature oxidation of materials that form volatile oxides has been mass transport limited, and hence fails to provide true chemically controlled rates. In initial experiments, reduction in sample length from 22 to 6 mm did appear to increase the observed rate of loss of oxygen atoms. For the data reported in Table I, sample length was reduced further to 1 mm. In calculating the ratios, R_T, the top photometer reading at 298°K was divided by the difference between the bottom photometer readings at temperature with the microwave discharge on and off. Thus, contributions to the bottom reading at temperature which may be due to background radiation from the hot graphite ring and/or oxygen atoms generated from oxygen molecules at the graphite surface have been subtracted out.

Temperature measurements were made using an optical pyrometer, sighting through the quartz tube and water jacket. The pyrometer readings were calibrated with a heated tungsten filament bulb, previously checked against a standard ribbon filament strip lamp. Initially, filament temperature as a function of power input to the bulb was measured in a bench setup (outside the tube and water jacket). The bulb was then inserted into the water cooled quartz flow tube and a plot of pyrometer reading vs. power input and hence true temperature was obtained. The correction was of the order of 200°C.

The most direct method of analyzing the data involves a determination of total oxygen atom loss rate. The measured light intensity I at

TABLE I: RATES OF TOTAL OXYGEN ATOM DECAY FOR CYLINDRICAL SAMPLES (0.082 cm long, 0.114 cm wall thickness)

A. $p_o = 3.07 \times 10^{-5}$ atm; $P = 4.15 \times 10^{-3}$ atm; $p_{O_2} = 2.10 \times 10^{-4}$ atm; $v_x = 2825$ cm/sec; $D = 56.5$ cm^2/sec; $Z = 3.58 \times 10^{-6}$ moles/cm^2-sec; $R_{Ag}/R_{Q,298} = 46.1$; $\gamma_{app,Ag} = 1.0$.

T, °K	R_{298}	R_T	$(G_T - G_{298})$ Moles/cm^2-sec (Equation 4)	γ_{app}
1600	1.26	2.78	2.52×10^{-6}	0.70
1603	1.35	3.16	2.46	.685
1615	1.54	3.00	1.83	.51
1840	1.21	2.58	2.52	.70
1890	1.63	5.47	2.50	.695
1902	1.53	4.31	2.44	.68
1970	1.51	4.11	2.43	.68
1970	1.25	2.69	2.48	.69
2050	1.29	3.89	3.00	.835
2200	1.21	3.78	3.26	.91
2270	1.41	4.14	2.71	.755
2325	1.31	3.90	2.94	.82
2470	1.27	3.45	2.87	.80
2730	1.50	4.34	2.52	.70
2760	1.48	3.67	2.34	.65
2800	1.52	3.91	2.32	.645

TABLE I (Continued): RATES OF TOTAL OXYGEN ATOM DECAY FOR CYLINDRICAL SAMPLES (0.082 cm long, 0.114 cm wall thickness)

B. $p_o = 9.68 \times 10^{-5}$ atm; $P = 8.20 \times 10^{-3}$ atm; $p_{O_2} = 1.55 \times 10^{-3}$ atm; $v_x = 970$ cm/sec; $D = 28.8$ cm^2/sec; $Z = 3.84 \times 10^{-6}$ moles/cm^2-sec.

T, °K	R_{298}	R_T	$(G_T - G_{298})$ Moles/cm^2-sec (Equation 4)	γ_{app}
1580	1.58	3.11	1.94×10^{-6}	.505
1722	1.29	3.19	2.89	.75
1970	1.29	2.88	2.68	.695
2141	1.40	3.30	2.58	.67
2283	1.40	2.59	2.04	.53
2665	1.64	3.88	2.20	.57
2665	1.92	5.05	2.02	.525

C. $p_o = 6.34 \times 10^{-5}$ atm; $P = 9.65 \times 10^{-3}$ atm; $p_{O_2} = 4.96 \times 10^{-4}$ atm; $v_x = 2740$ cm/sec; $D = 24.2$ cm^2/sec; $Z = 7.10 \times 10^{-6}$ moles/cm^2-sec.

1723	1.21	1.92	3.52×10^{-6}	.495
2050	1.17	2.07	4.35	.61
2430	1.17	2.03	4.19	.59

TABLE I (Continued): RATES OF TOTAL OXYGEN ATOM DECAY FOR CYLINDRICAL SAMPLES (0.082 cm long, 0.114 cm wall thickness)

D. p_o=9.26 x 10^{-6}atm; P=7.48 x 10^{-3}atm; p_{o_2}=5.60 x 10^{-4}atm; v_x=2725 cm/sec; D=31.4 cm^2/sec; Z=1.03 x 10^{-6} moles/cm^2-sec.

T,°K	R_{298}	R_T	(G_T-G_{298}) Moles/cm^2-sec (Equation 4)	γ_{app}
1580	1.89	5.23	0.605 x 10^{-6}	.59
1673	1.97	6.65	0.600	.58
2082	1.81	5.26	0.710	.69
2665	2.62	36.75	0.600	.58
2705	1.97	7.05	0.612	.59

E. p_o=3.80 x 10^{-5}atm; P=8.19 x 10^{-3}atm; p_{o_2}=1.88 x 10^{-3}atm; v_x=989 cm/sec; D=28.8 cm^2/sec; Z=1.54 x 10^{-6}moles/cm^2-sec; R_{Ag}/R_Q=40.6; γ_{app}=1.0.

1470	1.545	3.57	0.925 x 10^{-6}	.60
1723	1.585	3.92	0.946	.61
1740	1.542	4.10	1.013	.655
1987	1.455	4.17	1.12	.73
2030	1.60	4.96	1.06	.69
2080	1.51	5.91	1.24	.80
2242	1.60	6.15	1.16	.75
2435	1.585	3.87	0.936	.61
2440	1.50	3.93	1.04	.675

TABLE I (Continued): RATES OF TOTAL OXYGEN ATOM DECAY FOR CYLINDRICAL SAMPLES (0.082 cm long, 0.114 cm wall thickness)

F. (He) p_o=2.80 x 10^{-5}atm; P=4.15 x 10^{-3}atm; p_{o_2}=2.10 x 10^{-4}atm; v_x=2825 cm/sec; D=94.8 cm^2/sec; Z=3.13 x 10^{-6}moles/cm^2-sec; $R_{Ag}/R_{Q,298}$=51.6; γ_{app}=1.0.

T,°K	R_{298}	R_T	(G_T-G_{298}) Moles/cm^2-sec (Equation 4)	γ_{app}
1570	1.46	3.78	2.22 x 10^{-6}	.71
1890	1.39	5.94	2.92	.93
2050	1.44	7.00	2.92	.93

any point along the flow tube is proportional to oxygen atom concentration (0) at that point; i.e.,

$$I = k'(0) \tag{3}$$

The difference in photometer readings $(I_{Top}-I_{Bottom})$ is proportional to the total loss in oxygen atoms along the flow tube due to volume recombimation, surface recombination on quartz and graphite, and chemical reaction. Since the top photometer reading is independent at the temperature of the graphite, the difference between the bottom photometer readings at 298°K and at temperature $(I_{298}-I_T)_{Bottom}$ is proportional to the difference in total oxygen atom loss on graphite at 298°K and at temperature. The proportionally constant k' is $I_{Top}/(0)_{Top}$, where $(0)_{Top}$ was determined absolutely by NO_2 titration.[1] Hence the difference in total oxygen atom loss G at 298°K and at T°K in moles/cm^2-sec due to reaction and recombination on the graphite surface is given by:

$$(G_T - G_{298}) = \frac{(I_{298}-I_T)_{Bottom}(0)_{Top}}{I_{Top}} \left(\frac{v_x}{L}\right)\left(\frac{V}{A}\right)$$

$$= (0)_{Top}\left(\frac{1}{R_{298}} - \frac{1}{R_T}\right)\left(\frac{v_x}{L}\right)\left(\frac{V}{A}\right) \tag{4}$$

where (0) is in moles/cc, v_x is linear flow velocity in cm/sec, A = 0.48k cm^2 is sample surface area, L is sample length and $V = \pi r_o^2 L$. The values calculated from equation (4) are listed in Table I. Prior measurements of G_{298} in a straight flow tube established that it was less than 1% of (G_T-G_{298}) over the temperature range of interest.

The effect of oxygen atom pressure on the net atom loss rate is shown in Arrhenius plots in Figures 4 and 5 for paired sets of data taken under approximately constant conditions of total pressure, molecular oxygen pressure, and flow rate. In both cases, the reaction rate increases approximately linearly with oxygen atom pressure, p_o. There is a maximum in each of the atom loss curves, which shifts towards higher temperatures

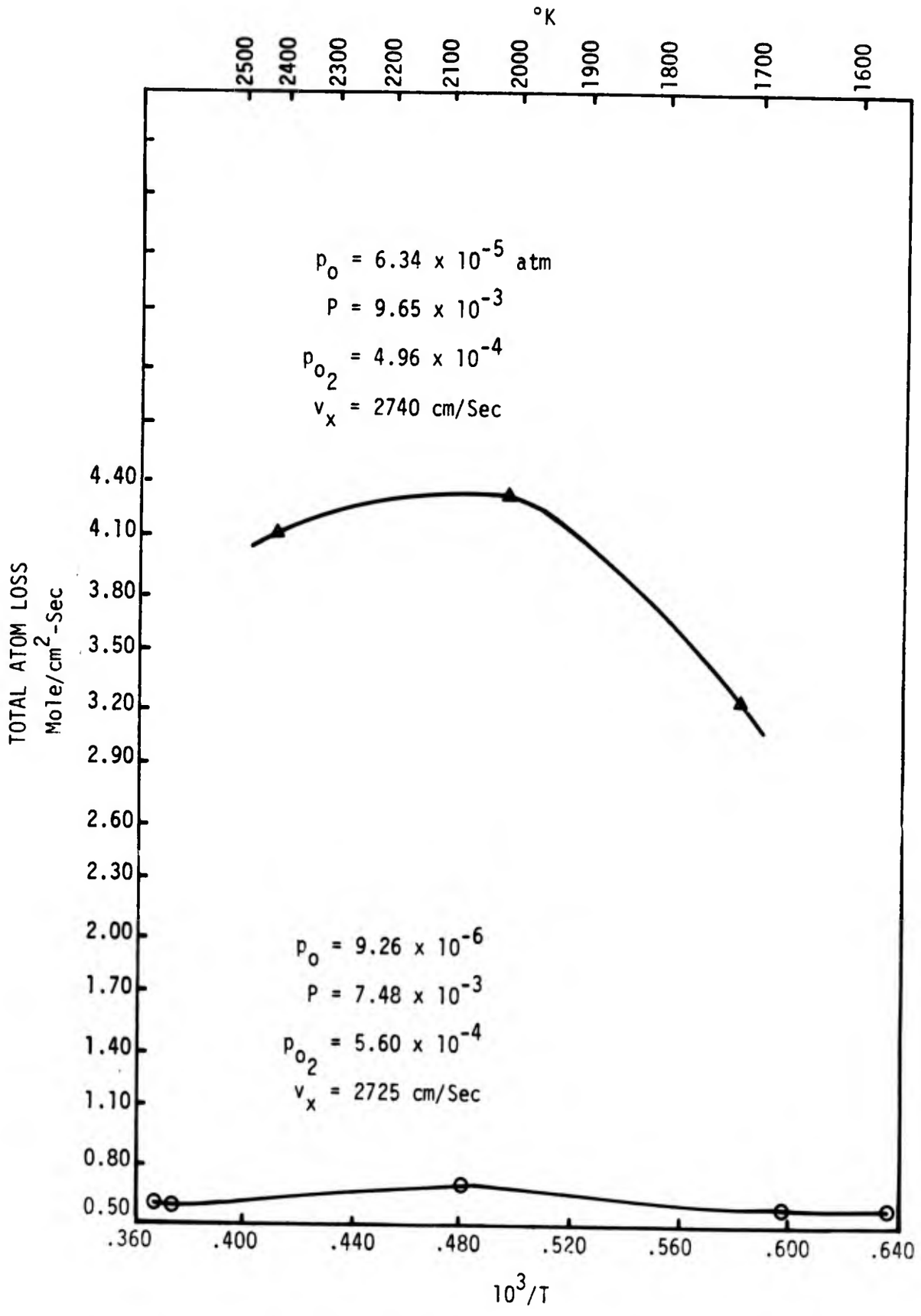

FIGURE 4: VARIATION OF NET ATOM LOSS RATE ON ATJ GRAPHITE SURFACES WITH ATOM PRESSURE UNDER FIXED FLOW AND DIFFUSION CONDITIONS (Linear Flow Velocity, 2733 ± 8 cm/Sec; Total Pressure, 8.57 ± 1.09 atm)

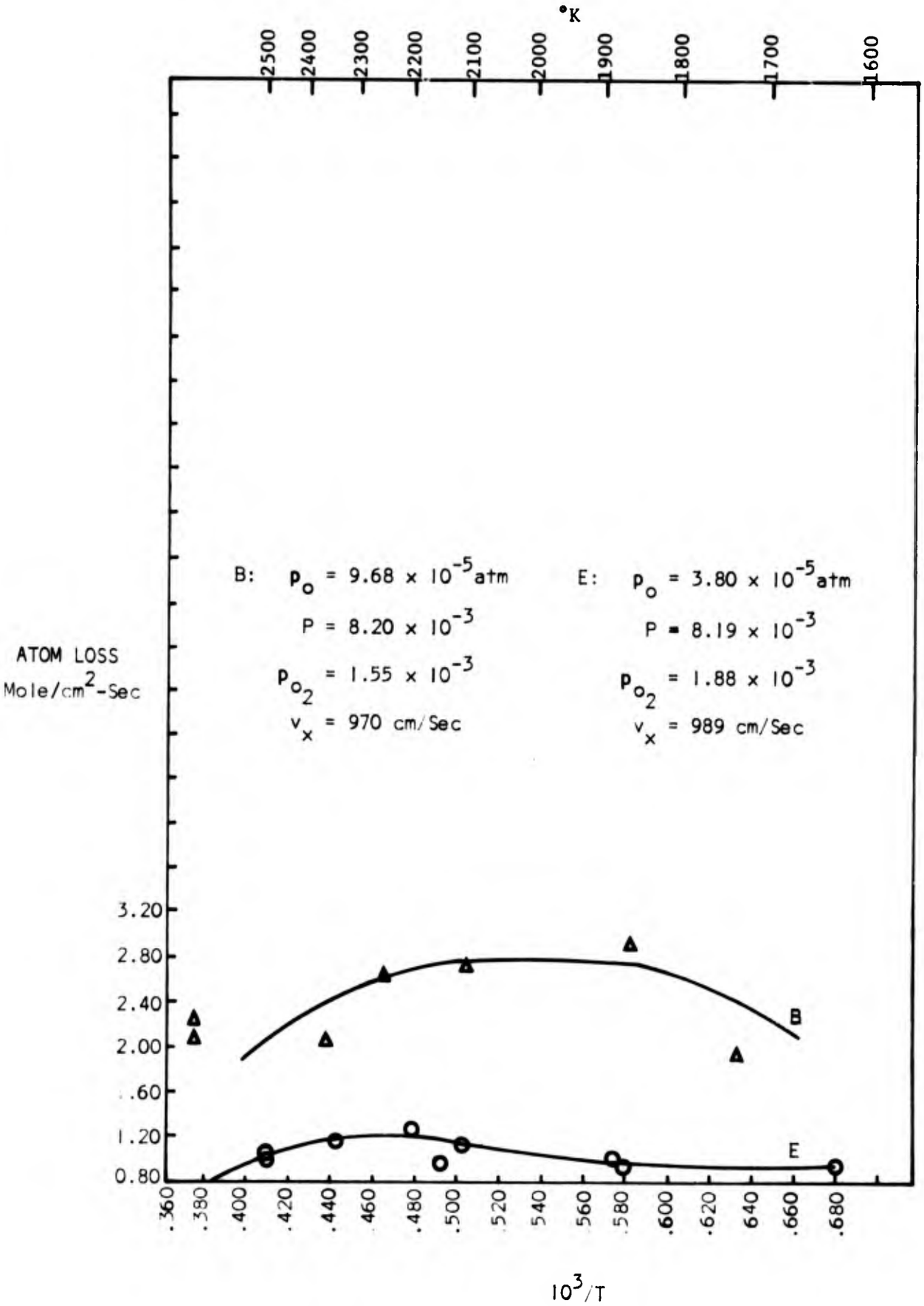

FIGURE 5: VARIATION OF NET ATOM LOSS RATE ON ATJ GRAPHITE SURFACES WITH ATOM PRESSURE UNDER FIXED FLOW AND DIFFUSION CONDITIONS (Linear Flow Velocity, 980 ± 10 cm/sec; Total Pressure, 8.2×10^{-3} atm)

with decreasing oxygen atom pressure. The maximum temperatures T_{max} are plotted vs. p_o in Figure 6; T_{max} varies approximately as $p_o^{-0.4}$. The collision rates, Z, and the collision efficiencies, γ_{app}, are discussed below.

For purposes of comparison, a silver ring sample of the same dimensions as the graphite was investigated in the fast flow apparatus under the pressure and flow conditions characteristic of data sets A, E, and F of Table I. The measured light intensity ratio for silver, R_{Ag}, which was found to be independent of temperature between 298 and 700°K, is compared to the ratio, R_Q, for the empty quartz tube in Table I. It is interesting to note that R_{Ag}/R_Q measured at 298°K was initially quite low, but immediately rose to the high values listed when the silver was heated. The ratio then remained at the high value, irrespective of temperature. The atom loss at the silver surface, due entirely to catalytic recombination, exceeds that at the ATJ surface by a factor of about 1.4.

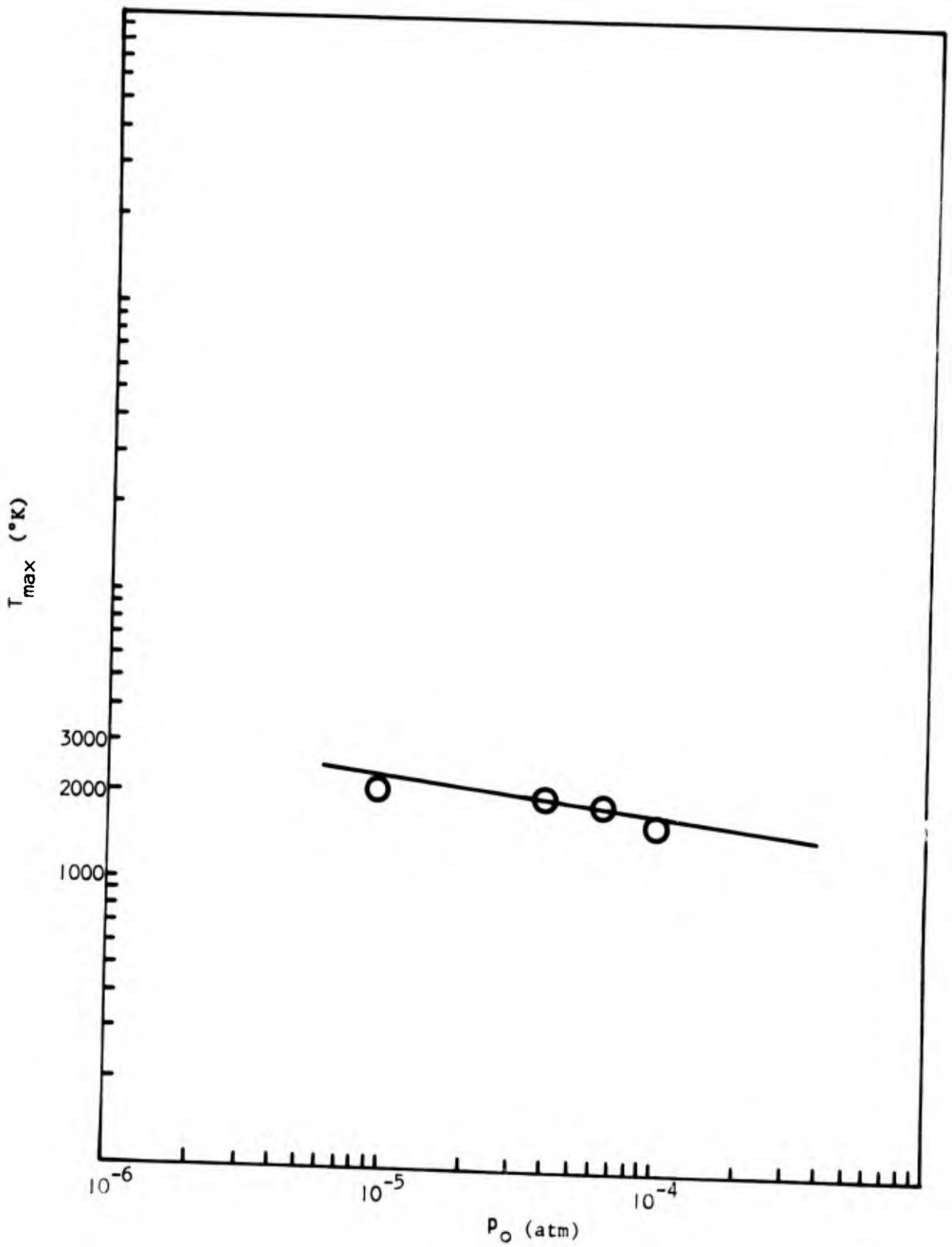

FIGURE 6: VARIATION OF THE TEMPERATURE OF MAXIMUM ATOM LOSS RATE WITH OXYGEN ATOM PRESSURE

III. WEIGHT CHANGE MEASUREMENTS

The fast flow experiments described above yield data on net interaction of oxygen atoms with the graphite surface. The net interaction is the sum of several components. Under steady state conditions, oxygen atoms which collide with the graphite surface can be desorbed as oxygen molecules (recombination), can react chemically with the graphite surface to form CO(g) or CO_2(g), and/or can be restituted to the gas phase as oxygen atoms. If ε is the fraction of oxygen atoms colliding with the surface which combine with the graphite to form CO(g) or CO_2(g), and γ is the fraction of oxygen atoms which are catalytically recombined to O_2, then γ_{app}, the net fraction of oxygen atoms interacting chemically with the surface, should be the sum of ε and γ.

$$\gamma_{app} = \gamma + \varepsilon \tag{5}$$

In order to determine both γ and ε from the previously derived net atom loss values, independent weight loss measurements were made in the fast flow system. Weight loss depends only on the chemical reaction to form CO(g) and CO_2(g) (ε), and is independent of atom recombination.

Reproducible weight loss measurements proved difficult to obtain due to the variability of the ATJ surfaces. In order to compensate in part for this variability, comparative weight loss measurements in molecular oxygen and in partially dissociated oxygen were made on the same sample in the neighborhood of a given temperature. A uniform surface pretreatment procedure, used for all samples, involved polishing with 40-101 emery paper and 600 grit SiC, followed by ultrasonic cleaning in methanol.

Weight change results are plotted in Figure 7. The open circles represent weight losses in g-atoms of C/cm^2-sec ac a molecular oxygen pressure $p_{O_2} = 2.10 \times 10^{-4}$ atm. The open triangles are the comparable weight losses in partially dissociated oxygen, $p_O = 3.07 \times 10^{-5}$ atm, $p_{O_2} = 2.10 \times 10^{-4}$ atm. For both sets of points the total pressure was 4.15×10^{-3} atm, with argon as the inert carrier. The average linear

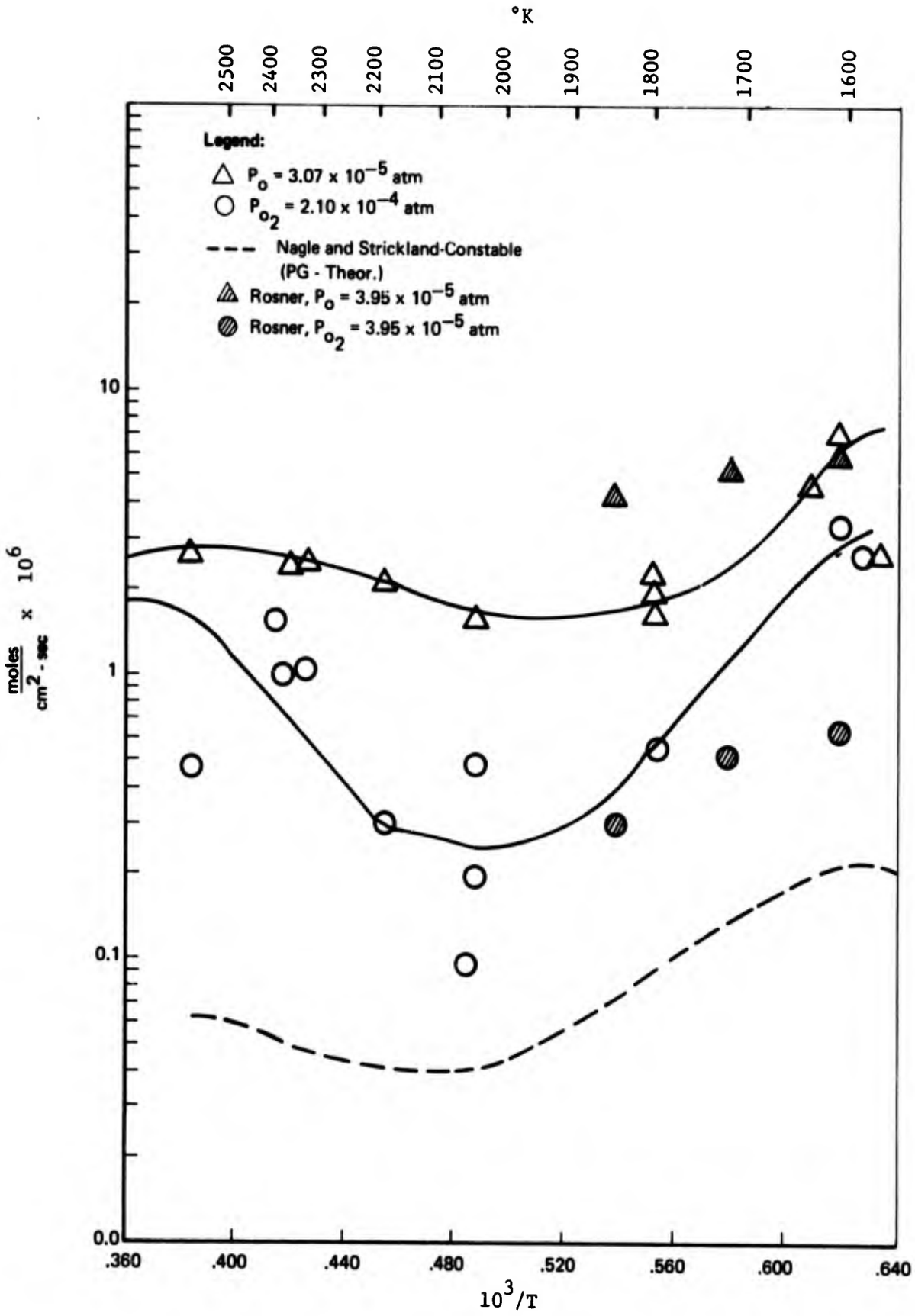

FIGURE 7: WEIGHT LOSSES IN UNDISSOCIATED AND PARTIALLY DISSOCIATED OXYGEN

flow velocity was 2825 cm/sec. The conditions correspond to those of data set A in Table I. The molecule results are obviously more variable than the atom results, a phenomenon also observed by Rosner and Allendorf for isotropic graphite.[4] It is possible that the atom reaction is less sensitive to precise surface condition than the molecule reaction. The semi-theoretical curve of Nagle and Strickland-Constable[3] for the reaction of pyrolytic graphite with molecular oxygen is also sketched in Figure 7. While our experimental results for ATJ fall above the semi-theoretical curve for PG as expected, both curves show a minimum at approximately the same temperature. The shaded points in Figure 7 were derived from Rosner and Allendorf's results on isotropic graphite.[4] Agreement is seen to be reasonably good over the small temperature range where the data overlap. The weight change differences derived from the curves drawn through the experimental data in Figure 7 are compared in Table II with net atom loss values determined under similar conditions, and calculated by means of equation (4).

The ditference between the total atom loss and the weight loss, assuming that the principal reaction product is CO(g), should represent atom loss due to recombination. From the data in Table II, it is clear that above 1840°K, the chemical reaction and the recombination reaction are of comparable importance. At the lowest temperatures investigated, near 1600°K, weight losses are quite high and of the same order of magnitude for both undissociated and partially dissociated oxygen. The incremental weight loss due to oxygen atoms is thus a small difference between two relatively large numbers, and is subject to substantial error.

TABLE II: WEIGHT OF LOSS OF ATJ GRAPHITE IN DISSOCIATED OXYGEN (CONDITIONS OF TABLE I, A)

T, °K	$10^3/T$	Wt. Loss Due to Atoms Moles/cm^2-sec (Figure 6)	Total Atom Loss Moles/cm^2-sec (Table I, A)	Atom Loss Due to Recombination Moles/cm^2-sec	γ	ε
1600	0.625	3.6×10^{-6}	2.52×10^{-6}	----	----	----
1603	.624	3.52	2.46	----	----	----
1615	.619	3.30	1.83	----	----	----
1840	.544	1.29	2.52	1.23×10^{-6}	0.34	0.36
1890	.529	1.29	2.50	1.21	0.34	0.36
1902	.526	1.31	2.44	1.13	0.32	0.37
1970	.508	1.31	2.43	1.12	0.31	0.37
1970	.508	1.33	2.48	1.15	0.32	0.37
2050	.488	1.43	3.00	1.57	0.51	0.47
2200	.454	1.79	3.26	1.47	0.41	0.50
2270	.441	1.91	2.71	0.80	0.22	0.53
2325	.430	1.96	2.94	0.98	0.27	0.55
2470	.405	1.71	2.87	1.16	0.32	0.48
2730	.366	0.88	2.52	1.64	0.46	0.25
2760	.362	0.79	2.34	1.55	0.43	0.22

IV. REACTION AND RECOMBINATION EFFICIENCIES

The weight loss and oxygen atom decay data have been presented in terms of linear reaction rates, representing total molar loss of oxygen atoms per cm^2 of geometric surface area per second. The rates refer to particular conditions of flow, total pressure, molecular oxygen partial pressure, and degree of dissociation. The variation of the absolute rates with flow velocity has already been noted, and may be due to large atom concentration gradients near the graphite surface induced by the high efficiency of oxygen atom reaction and recombination. In fact, when the surface reactivity is so high that more than one atom in a hundred colliding with the surface interacts with it, there is evidence from many sources[1], [5], [6], [7] that concentration gradients can be quite severe.

If the reaction rates measured relate to interactions at the surface, it might be anticipated that the fraction of atoms colliding with the surface which react chemically with graphite or which catalytically recombine on the surface, should be independent of the flow and total pressure parameters. However, determination of the collision frequency of atoms with the surface under the experimental conditions selected is not entirely straightforward. The kinetic theory expression based on oxygen atom partial pressure in the main gas stream certainly overestimates the collision frequency, since the partial pressure at the surface will be rapidly reduced below this value. The calculations presented in the Appendix of concentration as a function of radial and longitudinal distance in a tubular flow reactor cannot readily be used to interpret experimental data, even when reaction occurs entirely on the interior surface of a cylinder of the same internal diameter as the flow tube. The engineering correlation of Sherwood for vaporization and adsorption reactions in tubular flow reactors is not strictly applicable to the problem at hand.

It may be assumed that the collision rate, Z, is proportional to the product $(0)v_x$, the rate of arrival of oxygen atoms at the graphite

or silver surface, where (0) is the oxygen atom concentration (moles/cc) in the main gas stream in the neighborhood of the sample, as determined by NO_2 titration. Since some percentage of the atoms in the gas stream may never reach the walls, while others may make multiple collisions, Z might be smaller or larger than $v_x(0)$. If, in fact, $Z \approx (0)v_x$, then the calculated recombination coefficient for silver, based on the data in Table I, is unity within the limits of experimental error. Although silver may perhaps not be perfectly catalytic, there is no doubt that the literature value of 0.24[2] is low.[1] Finally, if the total atom loss results given in Table I are divided by Z, values of $\gamma_{app} = \gamma + \varepsilon$ are obtained, as listed in the fifth column of the Table.

For information, Table I includes values of the diffusion coefficient D estimated from the Gilliland equation:[8]

$$D = \frac{0.0043T^{3/2}\sqrt{\frac{1}{M_0} + \frac{1}{M_{av}}}}{P(V_0^{1/3} + V_{av}^{1/3})^2} \qquad (6)$$

where T was assumed equal to 298°K, M_0 is the molecular weight of atomic oxygen, M_{av} is the average molecular weight of the O_2-Ar or O_2-He carrier gas, P is total pressure in atmospheres, V_0 and V_{av} are molar volumes, estimated as 12.8 and 25.6 respectively. The observed rates do not appear to vary significantly with the value of D.

The γ_{app} values in Table I are plotted as a function of 1/T in Figure 8. Within experimental error average values of γ_{app} may be assigned as indicated by the solid line. Over the temperature range investigated, 1450-2900°K, the net reactivity of ATJ graphite exhibits a shallow maximum in the neighborhood of 2000°K for all of the data sets. At the maximum, about eight atoms in ten colliding with the surface either reacts chemically or recombines.

Individual γ and ε values were obtained from the weight loss and net atom loss data in Table II. The results are listed in columns 6 and 7 of the Table, and are plotted in Figure 9. The ε curve has a maximum and the

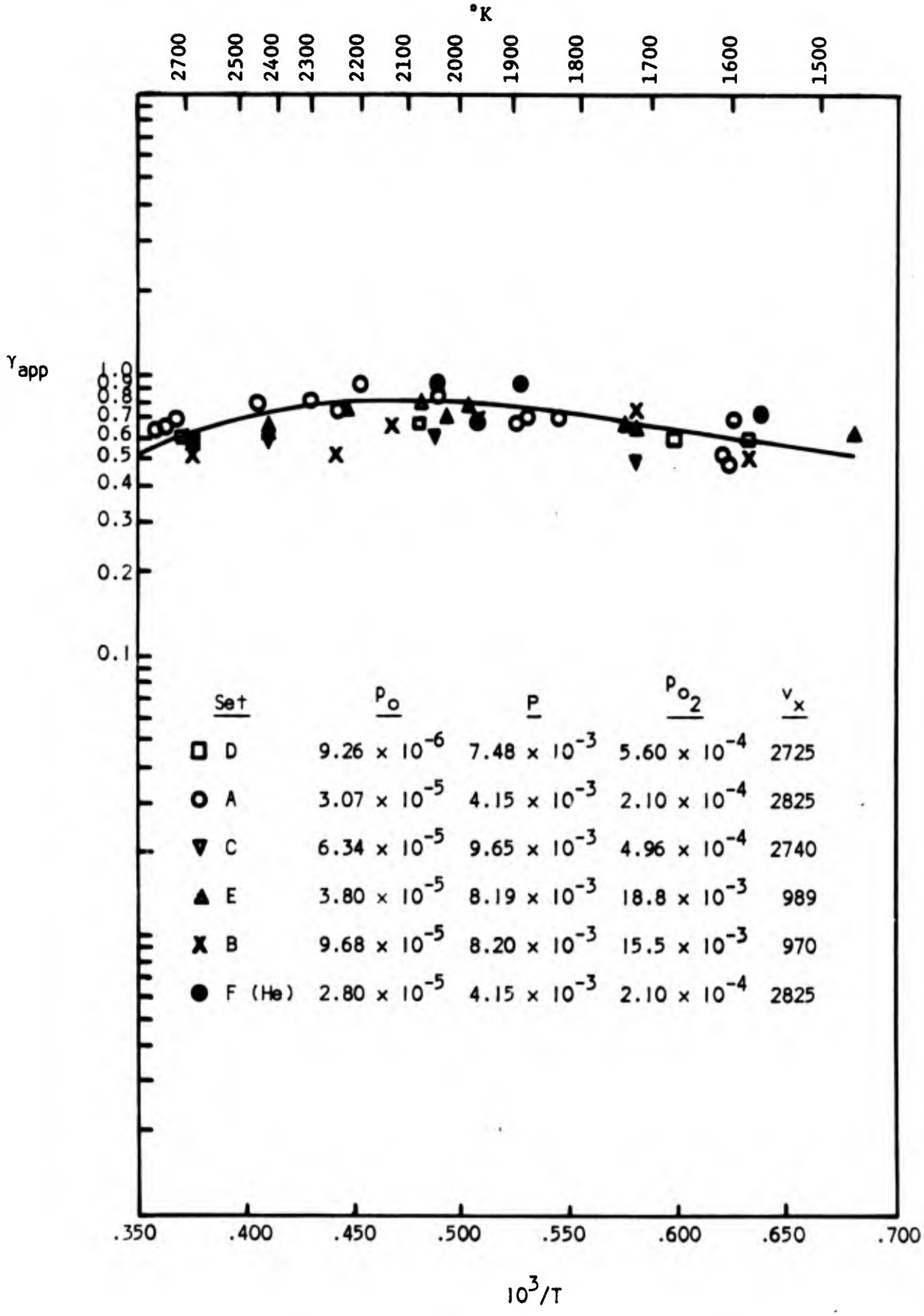

FIGURE 8: FRACTION OF ATOMS COLLIDING WITH ATJ GRAPHITE THAT INTERACT WITH THE SURFACE

γ curve has a minimum near 2300°K. As the temperature is increased from 2300 to 2900°K, the fraction of atoms combining chemically with graphite (ε) declines as the fraction recombining increases. In the absence of experimental data, one can only speculate about whether the trend would continue to higher temperatures. Between 1840 and 1970°K, about 70 atoms out of 100 interact with the graphite surface, 35 entering into the chemical reaction and 35 undergoing recombination.

The gas temperature in the experiments is unknown, but has been assumed to remain at 298°K. The rate of flow of oxygen atoms at a pressure of p_0 atm in a stream moving at 2000 cm/sec in a tube 1 cm in diameter is about 0.064 p_0 atoms/sec, compared to a kinetic theory collision frequency on a sample surface of 0.481 cm^2 of 0.31 p_0 collision/sec. Thus, even if every atom had access to the surface, it would make an average of less than 5 collisions during the time of traverse, hardly enough, it would seem to become thermally accommodated.

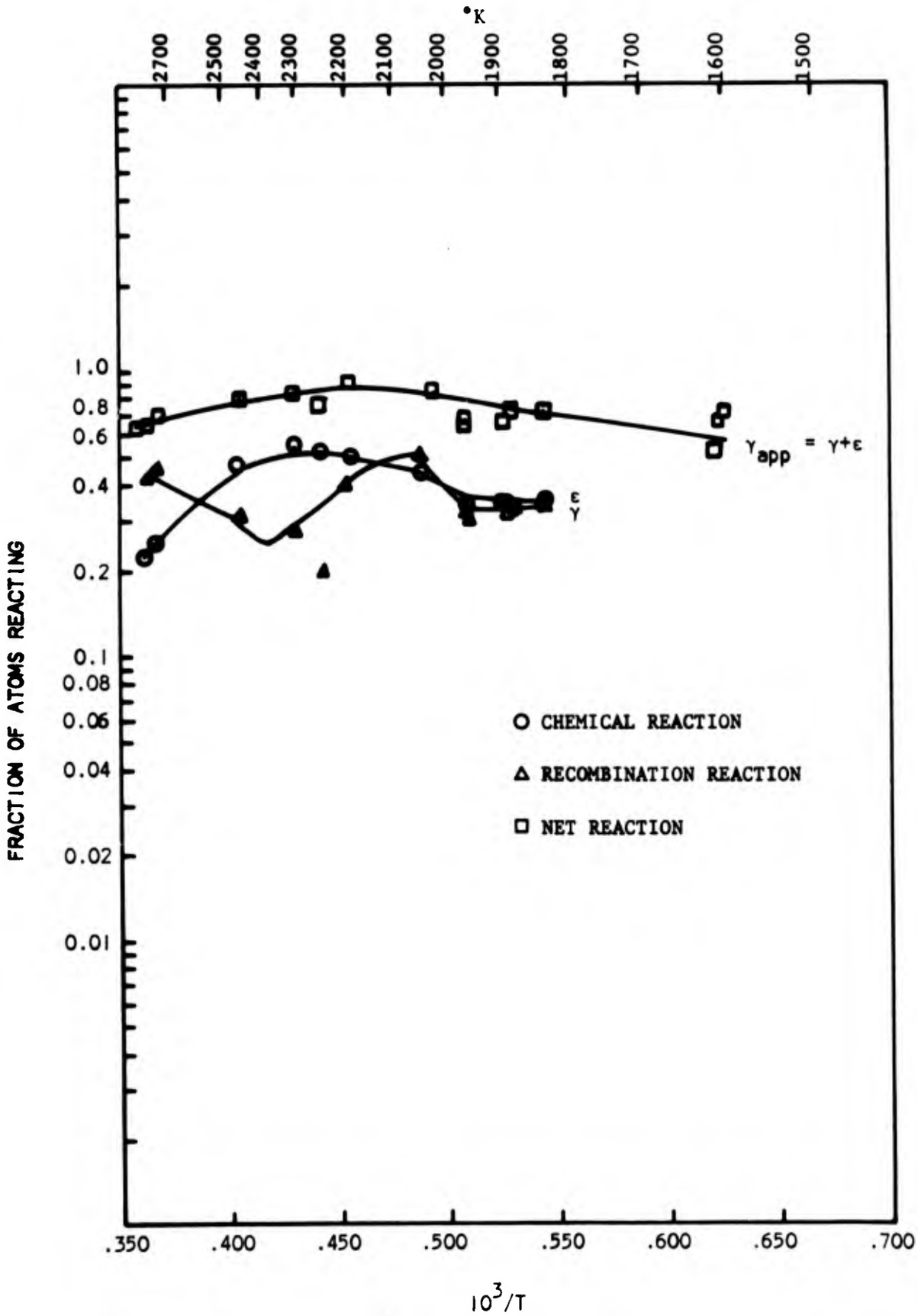

FIGURE 9: RECOMBINATION AND REACTION COEFFICIENTS AS A FUNCTION OF TEMPERATURE FOR ATJ GRAPHITE (p_o=3.07 x 10^{-5}atm)

V. MASS SPECTROMETER EXPERIMENTS

In the mass spectrometer experiments, a beam of partially dissociated oxygen impinges on a resistively heated ATJ sample in the vapor source region of a Nuclide Associates High Temperature Mass Spectrometer, Model HT-1. Vapor molecules leaving the graphite surface are collimated and mass analyzed by magnetic deflection. A movable shutter plate helps to distinguish gas molecules in the general background from those emanating directly from the heated graphite. A schematic diagram of the experimental arrangement is shown in Figure 10. A 50-50 mixture of molecular oxygen and argon at a total pressure of 3 to 6 torr expands through a fixed quartz leak, and is partially dissociated to atomic oxygen in a microwave discharge cavity, as described above for the fast flow experiments. Oxygen atom pressures were of the same order of magnitude. The quartz flow tube enters the vapor source region of the mass spectrometer through a vacuum seal, and is bent to direct a beam of gas onto the surface of a resistively heated sample of ATJ graphite. The graphite surface lies parallel to the shutter plate separating the vapor source from the ion source region of the mass spectrometer.

Experiments were run at a series of increasing temperatures between 413 and 1229°K as measured with a Pt-Rh thermocouple tightly held in a depression on the back face of the graphite. Ion intensities for ions exhibiting a shutter profile were measured with the microwave discharge off and on. When the discharge is off, a stream of molecular oxygen and argon impinges on the graphite surface. When the discharge is on, with no change in total flow rate, some of the oxygen molecules are dissociated to atoms. Results are summarized in Table III. The O^+ signal, which did show a shutter profile, is not recorded since it is strongly influenced by fragmentation of O_2. It did show a very small decline when the microwave was turned on, due to the decline in the molecular oxygen concentration. However, due to the simultaneous production of oxygen atoms, O^+ did not decline nearly as much as O_2^+. Those experiments

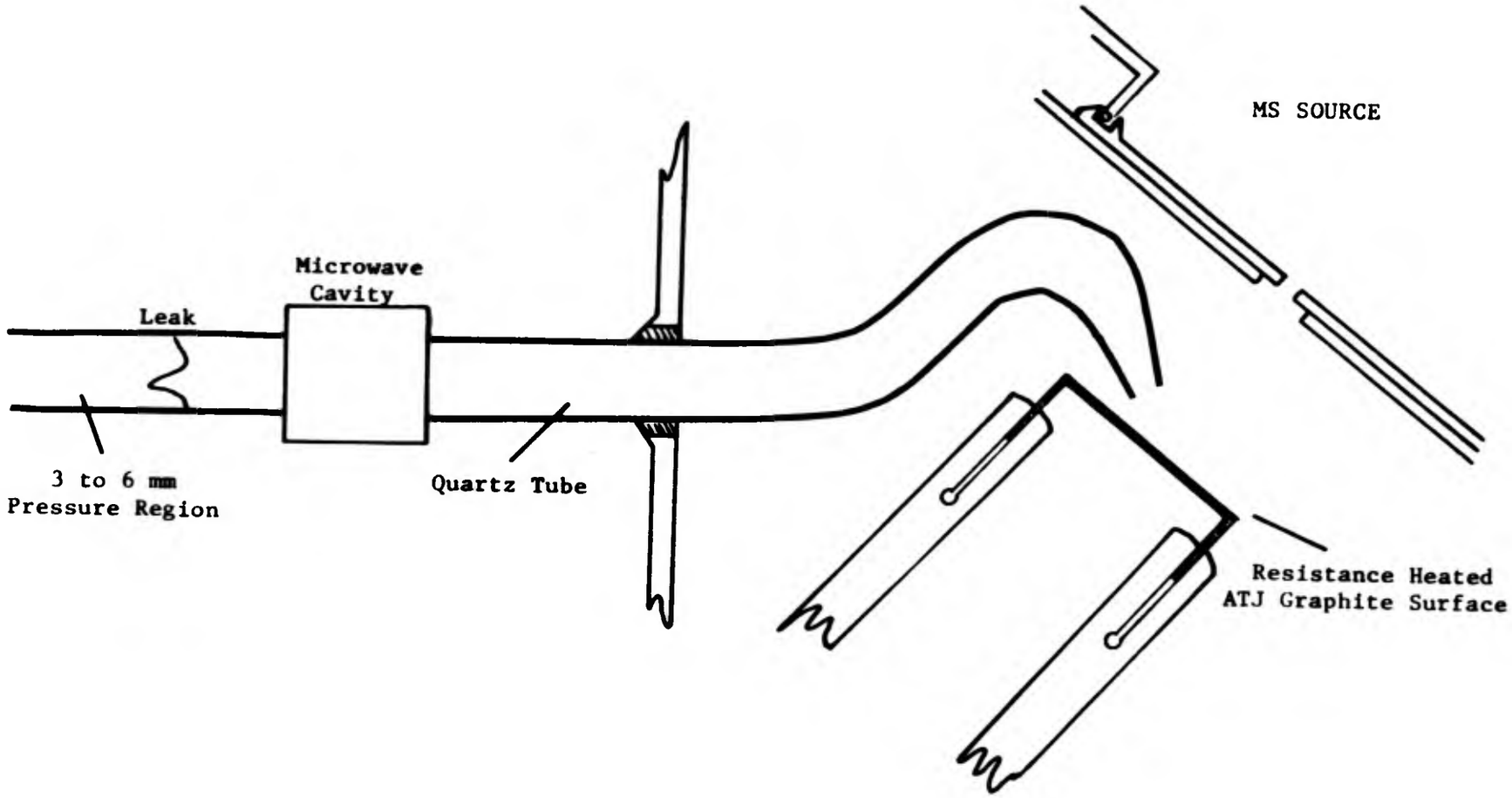

FIGURE 10: SCHEMATIC DIAGRAM OF APPARATUS FOR OXYGEN ATOM RECOMBINATION STUDIES IN MASS SPECTROMETER

TABLE III: EFFECT OF ATOMIC OXYGEN THROUGH SPECIES DISTRIBUTION FROM ATJ GRAPHITE

T, °K	Species	I^+, Arbitrary Units		Intensity Change When Gas is Dissociated
		Microwave Off	Microwave On	
413	O_2^+	786	750	-36
	CO^+	16.8	16.8	0
	CO_2^+	4.1	6.2	+2.1
	Ar^+	318	318	0
	NO^+	0.24	0.9	+0.66
610	O_2^+	795	780	-15
	CO^+	23	23	0
	CO_2^+	6.2	7.9	+1.7
	Ar^+	316	316	0
	NO^+	0.21	0.94	+0.73
770	O_2^+	870	855	-25
	CO^+	27	37	+10
	CO_2^+	8.1	9.3	+1.2
	Ar^+	345	345	0
	NO^+	0.28	1.16	+0.88

(Continued)

TABLE III (Continued): EFFECT OF ATOMIC OXYGEN THROUGH SPECIES DISTRIBUTION FROM ATJ GRAPHITE

T, °K	Species	I^+, Arbitrary Units		Intensity Change When Gas is Dissociated
		Microwave Off	Microwave On	
925	O_2^+	831	816	-15
	CO^+	83.1	95.1	+12
	CO_2^+	13.2	14.3	+1.1
	Ar^+	349	349	0
	NO^+	0.4	1.32	+0.92
1119	O_2^+	756	744	-12
	CO^+	230	246	+16
	CO_2^+	14.6	15.2	+0.6
	Ar^+	348	348	0
	NO^+	0.66	1.53	+0.87
1229	O_2^+	724	710	-14
	CO^+	312	328	+16
	CO_2^+	14.8	15.2	+0.4
	Ar^+	343	343	0
	NO^+	0.9	1.8	+0.9

were done with 60 ev ionizing electrons. With 17 ev electrons, the O^+ signal shows a sharp increase when the microwave is turned on. The decline in the O_2^+ signal when the microwave is turned on probably does roughly reflect the number of oxygen molecules that have undergone dissociation. The amount of carbon removed from the surface as CO(g) or CO_2(g) is clearly enhanced in the presence of oxygen atoms, compared to the undissociated gas over the entire temperature range investigated. The degree of enhancement increases roughly with the temperature. The net carbon removal rate increases strongly with temperature for both the undissociated and partially dissociated gas streams. The sum of the CO^+ and CO_2^+ ion signals for the dissociated gas streams are plotted vs. 1/T in Figure 11. The changes in product distribution with temperature and dissociation are quite interesting. The CO^+ signal increases continuously with temperature for both the undissociated and partially dissociated reactant gas beams. The CO_2^+ signal also increases with temperature at the lower part of the temperature range studied but begins to level off at the higher temperatures. Up to 610°K, the effect of dissociation is to increase the CO_2^+ signal. Above 610°K, dissociation increases the CO^+ signal far more than the CO_2^+ signal. The CO^+/CO_2^+ ratio for both the undissociated and partly dissociated reactant is plotted vs. 1/T in Figure 12. The NO^+ peak is unexplained. In initial trials it was associated with a leak in one of the flanges to the vapor source region. While the NO^+ ion intensity increased when the microwave was turned on, the NO did not appear to be introduced through the oxygen-argon beam line. The leak in the flange was repaired, and the NO^+ ion intensity declined, but some signal did persist as indicated in the Table.

The experiments described were limited in temperature due to the formation of a low melting eutectic at the point of contact between graphite and the stainless steel support rods and current carrying leads. While extrapolation of low temperature data over a wide interval is always risky, it is particularly so for the graphite-oxygen system, which displays many anomalies with temperature. Nonetheless, the mass spectrometer results do lend support to the assumption, used above, that CO(g) is the major product of the C(s)-O(g) reaction.

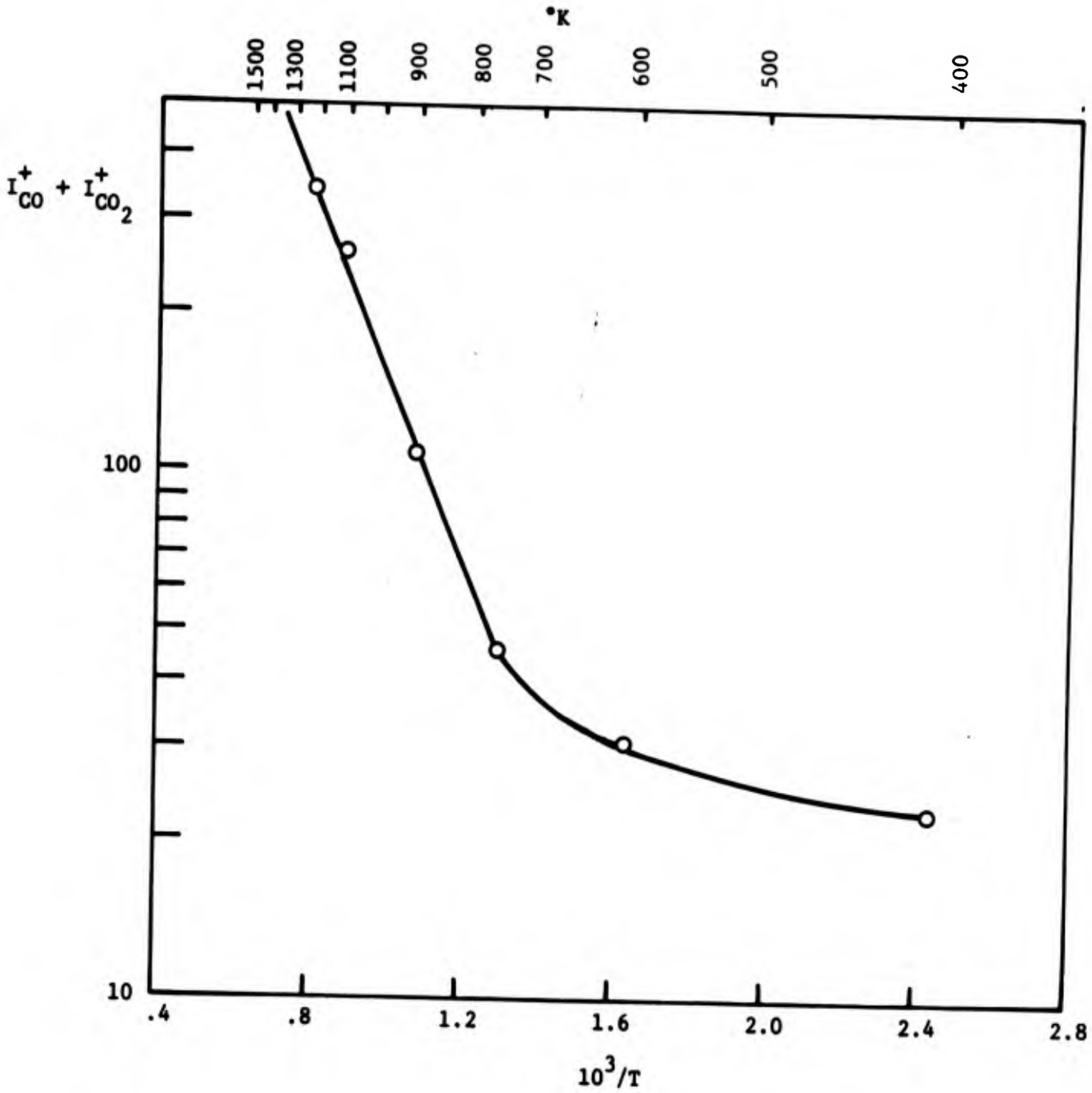

FIGURE 11: $(CO^+ + CO_2^+)$ vs. 1/T FOR DISSOCIATED OXYGEN

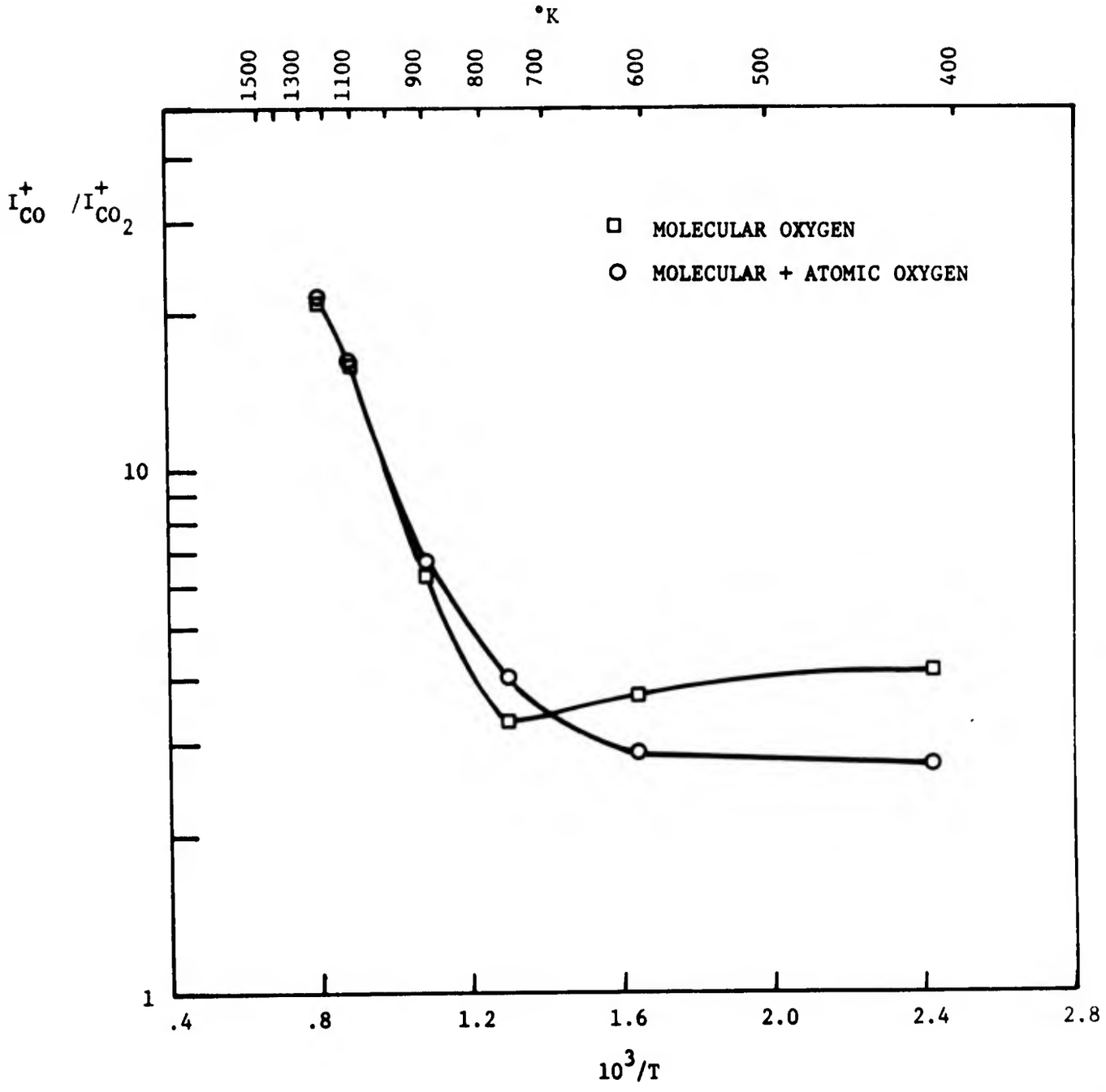

FIGURE 12: CO^+/CO_2^+ FOR DISSOCIATED AND UNDISSOCIATED OXYGEN

VI. DISCUSSION AND CONCLUSIONS

A. Summary of Experimental Results

Under the current program, the interactions of graphite with molecular and atomic oxygen have been investigated over the temperature range 1600-2800°K, at atom partial pressures of 7.0×10^{-3} to 7.4×10^{-2} torr and molecular oxygen pressures of 0.16 to 1.4 torr. Previous work on the oxidation of graphite by atomic oxygen had been carried out to 2100°K, and was confined only to measuring a rate of recession. Under reentry conditions, both mass transport in the form of materials' recession and heat transport must be considered. When an oxygen atom collides with and becomes adsorbed on a graphite surface, it may be desorbed as CO(g), CO_2(g), or O_2(g), or it may be restituted to the gas phase essentially unchanged. Desorption in combination with graphite leads to materials' recession (weight loss) as well as heat transport; desorption of O(g) as O_2(g) contributes only to the heat transport, and is not reflected in a weight change. In order to assess the total extent of the interaction between graphite and atomic oxygen, three types of experiments were carried out: (1) fast flow experiments in a tubular reactor in which total oxygen atom decay due to chemical reaction and catalytic recombination was measured; (2) fast flow experiments in the same reactor with measurement of weight change (chemical reaction only) in undissociated and partially dissociated oxygen; and (3) mass spectrometric experiments in which the CO/CO_2 product distribution was measured. The major findings may be summarized as follows for the experimental conditions employed:

(1) The rate of net atom loss due to recombination and chemical reaction on the graphite surface is constant (independent of time) under steady state conditions of oxygen atom partial pressure.

(2) The rate of net atom loss on graphite is approximately first order in oxygen atom partial pressure.

(3) There is a pressure dependent maximum in the net rate of atom loss with temperature, the maximum shifting from 2270°K at $p_O = 9 \times 10^{-6}$ atm to 1850°K at $p_O = 9 \times 10^{-5}$ atm.

[redacted]

(4) The rate of graphite recession in undissociated oxygen at a pressure of 2×10^{-4} atm has a minimum in the neighborhood of 2040°K.

(5) In partially dissociated oxygen, with $p_o = 3 \times 10^{-5}$ atm and $p_{o_2} = 2 \times 10^{-4}$ atm, the incremental weight loss due to oxygen atoms has a maximum near 2300°K. In the neighborhood of the maximum, the fraction of atoms catalytically recombining is at a minimum. Near 2800°K, where about 65% of the atoms colliding with the surface interact, approximately 22% react chemically and 43% undergo catalytic recombination to O_2. Between 1840 and 1970°K, where about 71% of the collisions lead to oxygen atom decay, the distribution is roughly 37% leading to chemical reaction and 34% resulting in catalytic recombination.

(6) The major product of the chemical reaction between graphite and atomic or molecular oxygen in the temperature and pressure range investigation is probably CO(g).

B. Reaction Mechanism

The common occurrence of maxima and minima in Arrhenius curves for graphite-oxygen interactions makes extrapolation to conditions outside of the experimental range particularly difficult. In the presence of non-equilibrium concentrations of oxygen atoms, the competitive processes of chemical reaction and catalytic recombination complicates the situation still further. If individual steps leading to reaction and recombination can be isolated, and reaction rates assigned, much more reliable extrapolations become possible.

Nagle and Strickland-Constable[3] have proposed a mechanism for the chemical reaction between graphite and molecular oxygen and have assigned rate constants empirically to fit existing data on the oxidation of pyrolytic graphite over a very wide range of O_2 pressures, from 2.5×10^{-5} to 0.23 atm. The mechanism is based on Langmuir adsorption at two types of sites, designated as Type A and Type B, on the graphite surface. The nature of the sites has never been well-defined, although recent LEED

and field ion microscopy experiments certainly support the concept of there being many different types of adsorption sites on any surface. If CO(g) is the only product of the graphite-oxygen reaction at high temperatures, then, according to the mechanism proposed,[3] oxygen molecules may adsorb on A sites and desorb as CO(g), leaving a bare A site; oxygen molecules may adsorb on B sites and desorb as CO(g), leaving bare A sites; and finally A sites may be transformed into B sites by an activated process. The various steps in the mechanism are summarized in the following equations:

$$A + O_2 \xrightarrow{k_a} A \ldots O_2(ads) \qquad (a)$$

$$A \ldots O_2(ads) \xrightarrow{k_b} A + 2CO(g) \qquad (b)$$

$$B + O_2 \xrightarrow{k_c} B \ldots O_2(ads) \qquad (c)$$

$$B \ldots O_2 \xrightarrow{k_d} A + 2CO(g) \qquad (d)$$

$$A \xrightarrow{k_e} B \qquad (e)$$

If the A sites are strongly binding, and the B sites are weakly binding towards molecular oxygen, then if x is the fraction of the surface covered by A sites and θ_A is the fraction of these which are filled, a Langmuir treatment of the A sites leads to the following expressions for the rate of formation of CO(g) from A sites, $\frac{d(CO)A}{dt}$:

$$\frac{d(CO)A}{dt} = k_b(x\theta_A)$$

$$\frac{d(x\theta_A)}{dt} = 0 = k_a(x-x\theta_A)\, p_{O_2} - k_b(x\theta_A)$$

$$\frac{d(CO)_A}{dt} = \frac{k_a k_b p_{O_2} x}{k_b + k_a p_{O_2}} = \frac{k_a p_{O_2} x}{1 + k_z p_{O_2}}$$

A similar treatment for adsorption and desorption at B sites leads to the expressions:

$$\frac{d(CO)_B}{dt} = k_d[(1-x)\theta_B]$$

$$\frac{d[(1-x)\theta_B]}{dt} = 0 = k_c(1-x)(1-\theta_B)p_{O_2} - k_d(1-x)\theta_B$$

$$\theta_B = \frac{k_c p_{O_2}}{k_d + k_c p_{O_2}} \qquad k_d >> k_c \quad \frac{k_c p_{O_2}}{k_d}$$

$$\frac{d(CO)_B}{dt} = k_c p_{O_2}(1-x)$$

Thus, the net rate of formation of CO will be given by:

$$\frac{d(CO)}{dt} = \frac{k_a p_{O_2} x}{1 + k_z p_{O_2}} + k_c p_{O_2}(1-x)$$

Applying a steady state approximation to the fractional coverage x, we find:

$$\frac{d(x)}{dt} = k_c(1-x)p_{O_2} - k_e x = 0$$

$$x = \frac{k_c p_{O_2}}{k_e + k_c p_{O_2}} = \frac{1}{1 + \dfrac{k_e}{k_c p_{O_2}}}$$

The rate constants adopted by Nagle and Strickland-Constable to give rates of reaction with PG in moles/cm^2-sec, with pressure in atmospheres, are:

$$k_a = 20e^{-30,000/RT}$$

$$k_c = 4.46 \times 10^{-3} e^{-15,200/RT}$$

$$k_e = 1.51 \times 10^5 e^{-97,000/RT}$$

$$k_z = k_a/k_b = 21.3e^{+4100/RT}$$

Of course, with other grades of graphite, the constants would have to be appropriately scaled, but the general behavior should be similar.

An analogous mechanism should certainly apply to the reaction of graphite with atomic oxygen in the same temperature range, with the possibility for recombination taken into account. However, a problem immediately arises with respect to the assignment of rate constants. The rate constant k_a applies to the adsorption of O_2 molecules on the strongly binding Type A sites. The kinetic theory expression for the number of oxygen molecules colliding with the surface is $(\frac{1}{4})(\frac{p}{RT})(\bar{w})$ where $\bar{w}$, the average velocity of O_2 molecules has a value of 298°K of 4.43×10^4 cm/sec. The pre-exponential factor associated with k_a would not be expected to exceed $\bar{w}/4RT$, which is equal to 0.453 at 298°K, and is somewhat smaller at higher temperatures. The pre-exponential factor of 20 chosen by Nagle and Strickland-Constable to give a "best fit" to their PG data is thus far too large to justify on simple theoretical grounds. The pre-exponential factor of 4.46×10^{-3} associated with k_c, the rate constant for adsorption on Type B sites, is quite reasonable on the basis of kinetic theory, assuming a sticking coefficient of about 10^{-2}.

If the Nagle and Strickland-Constable model is assumed to hold for the reaction between graphite and atomic oxygen, the rate constants might be assigned as follows. The adsorption of oxygen atoms on Type A sites might be assumed to be unactivated with a sticking probability of unit, giving $(k_a)_0 = 0.453$. The adsorption of oxygen on Type B sites might also be unactivated with a sticking probability of 10^{-2}, giving $(k_c)_0 = 4.46 \times 10^{-3}$. If the reaction step (b) is the same for atoms and molecules, then $(k_b)_0 = k_b = 0.94e^{-34,100/RT}$. The rates calculated on this basis for atom and molecule pressures of 3×10^{-5} atm are compared in Figure 13. The reaction rates in the atomic oxygen

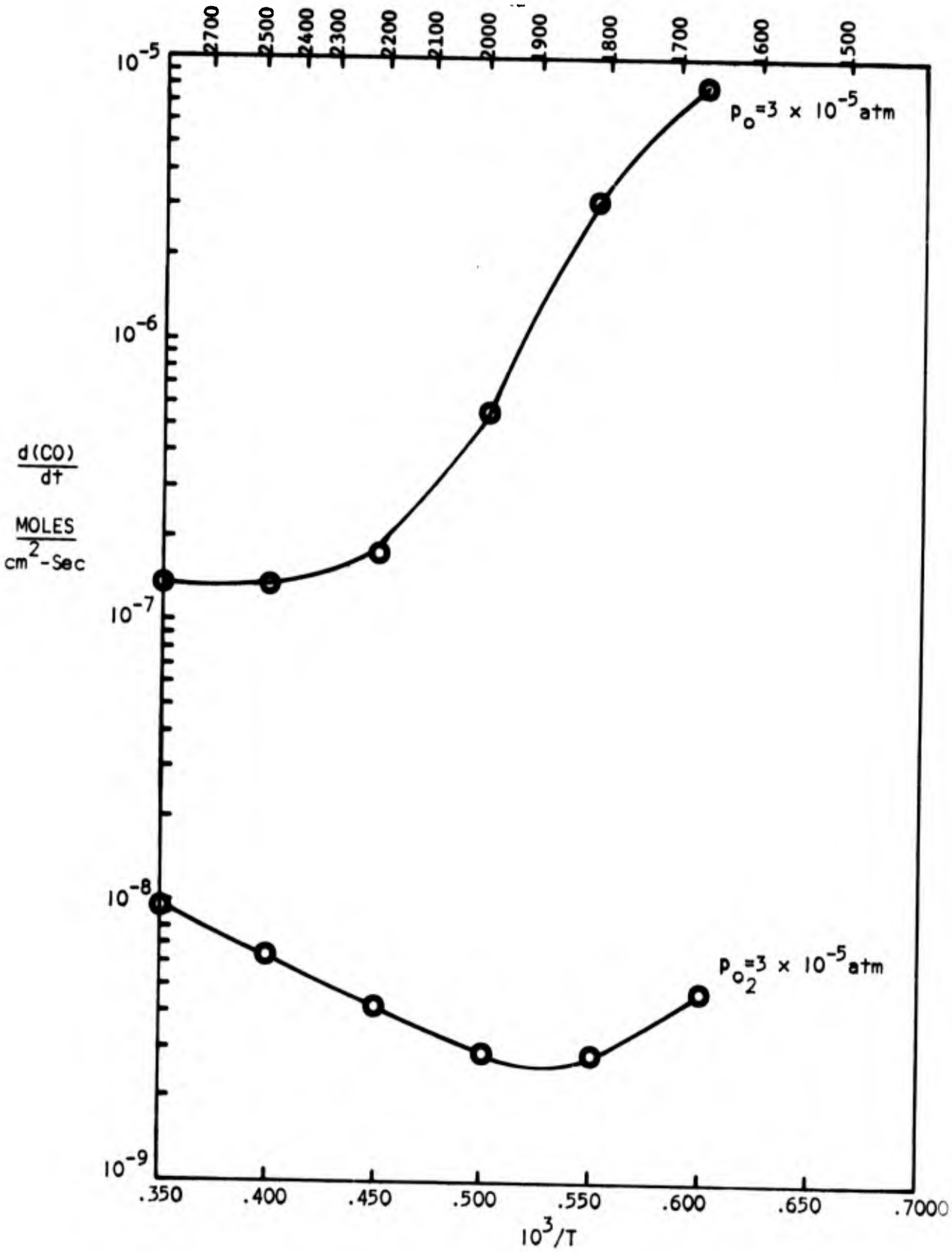

FIGURE 13: OXIDATION RATE PREDICTIONS BASED ON THE NAGLE AND STRICKLAND-CONSTABLE MODEL

are predicted to be very much higher than the corresponding rates in molecular oxygen. However, the degree of acceleration is very much higher than that which has been observed experimentally. Furthermore, the very sharp drop in atom reactivity with increasing temperature in the lower temperature regime is completely contrary to experience. The equation used to calculate the rates of reaction in atomic oxygen is:

$$\frac{d(CO)_o}{dt} = \frac{0.453\ p_o x}{1 + 0.48e^{34,100/RT} p_o} + 4.46 \times 10^{-3} p_o (1-x)$$

$$x = \frac{1}{1 + \frac{3.38 \times 10^{7} e^{-97,000/RT}}{p_o}}$$

The denominator of the first term remains very close to unity at all temperatures for the low atom partial pressures. The fractional coverage x is essentially zero for $0.350 \leq 10^3/T \leq 0.450$. In this range, therefore:

$$\frac{d(CO)_o}{dt} \approx 4.46 \times 10^{-3} p_o \qquad 0.350 \leq \frac{10^3}{T} \leq 0.450$$

For $10^3/T \geq 0.550$, the first term essentially controls the rate and hence:

$$\frac{d(CO)_o}{dt} \approx \frac{0.453\ p_o}{1 + (3.38 \times 10^{7} e^{-97,000/RT}/p_o)}$$

For very low temperatures, as x approaches unity, the reaction rate would be predicted to level off at approximately $0.453\ p_o$.

The discrepancy between theory and experiment might be resolved if the adsorption of oxygen atoms on Type A sites were activated, or if the sticking probability for adsorption were less than one and

strongly temperature dependent. As was pointed out above, the kinetics of adsorption of molecules on Type A sites is also very much an open question. Since adsorption must precede any surface reaction, and may even be a controlling factor in the overall kinetics, a simultaneous experimental and theoretical approach to the problems would be of great value for the establishment of useful predictive reaction mechanisms. Once the adsorption mechanism is well-defined, the competition between chemical reaction and catalytic recombination can be assessed much more readily.

C. Design Implications

From a practical point of view, it appears from the present work that a decline in the rate of the chemical reaction at high temperatures is associated with an increase in the rate of recombination. Thus, while mass transport problems may be diminished, heat transport problems will not be.

The recombination reaction:

$$O(g) \xrightarrow[\text{surface}]{\text{graphite}} 1/2\ O_2(g)$$

is exothermic by 61.0 kcal/mole at 2000°K.[9] The chemical reaction:

$$O(g) + C(s) \longrightarrow CO(g)$$

is exothermic by 89.4 kcal/mole at the same temperature. If a significant concentration of oxygen atoms persist to the surface of a reentry vehicle, the probability that they will react or recombine on the surface is exceedingly high. Sixty to ninety percent of the atoms colliding with the surface will interact, with high associated heat transfer. Experimentally, the chemical and recombination reactions are of comparable importance. In undissociated air or oxygen, the sole reaction which occurs:

$$1/2\ O_2(g) + C(g) \longrightarrow CO(g)$$

releases only 28.4 kcal/mole at 2000°K, considerably less than either oxygen atom reaction. It is thus clear that the presence of a non-equilibrium concentration of oxygen atoms at the surface of a reentry vehicle cannot be ignored in heat transport calculations.

The question arises as to what the oxygen atom concentration will be in the neighborhood of a surface under various conditions of practical importance. In "frozen flow," it is assumed that all atoms generated in the shock wave reach the surface of the vehicle, and that no recombination occurs in the gas phase. At the other extreme of equilibrium flow, homogeneous gas phase recombination rates are assumed to be extremely rapid. The heat transfer due to heterogeneous oxygen atom reactions is of course of greatest importance in frozen flow. In most cases of real interest, it is likely that neither the frozen flow nor the equilibrium flow approximation is valid.

The tendency for the boundary layer to become frozen depends on the ratio of the diffusion time for an atom across the boundary layer to the time required for homogeneous atom recombination within the boundary layer. If the ratio is low, atoms will diffuse to the surface faster than they can recombine in the gas, and frozen flow will be approached. The ratio in question varies roughly as $p_s^2/T_s^{3.5}$ where p_s is the pressure at the stagnation point on the external flow at T_s is the absolute temperature at the same point.[10] Thus, frozen flow is favored by low stagnation pressures and high stagnation temperatures.

Wind tunnel experiments under simulated frozen flow conditions[11][12][13] confirm the anticipated large effects of efficient surface recombination on heat transfer. Thus, for silver and copper surfaces, which are essentially perfect recombination catalysts ($\gamma \simeq 1$), the measured heat transfer is 30-40% higher than for poorly catalytic surfaces ($\gamma < 10^{-4}$). Since graphite interacts strongly and exothermically with dissociated oxygen, heat transfer calculations that fail to take into account oxygen atom recombination and reaction can be grossly in error.

APPENDIX

EFFECTS OF RADIAL DIFFUSION IN THE FAST FLOW SYSTEM

The general problem of chemical reaction and diffusion in a fast flow system with catalytic walls has been analyzed by Walker.[6] The differential equation defining ψ, the mole fraction of oxygen atoms in the gas stream, in terms of radial distance r and distance along the flow tube, z, is as follows:

$$2U\left(1-\frac{r^2}{r_o^2}\right)\frac{\partial\psi}{\partial z} - D\left(\frac{\partial^2\psi}{\partial r^2}+\frac{1}{r}\frac{\partial\psi}{\partial r}+\frac{\partial^2\psi}{\partial z^2}\right) = -k_v\psi \qquad (1)$$

subject to the boundary conditions:

$$\psi = \psi_o \text{ at } z = 0$$

$$\psi = 0 \text{ at } z = \pm\infty$$

$$\left(\frac{\partial\psi}{\partial r}\right)_{r=R} = -\psi/r_o\delta$$

where U is average linear flow velocity in the direction of the gas stream; Poiseuille flow is assumed; D is the diffusion coefficient for oxygen atoms in the gas mixture; k_v is the rate constant for homogeneous recombination expressed as a first order rate constant; r_o is the radius of the flow tube; and $\delta = 4D(1-\gamma/2)/\bar{w}\gamma r_o$, where γ is the recombination coefficient and $\bar{w}$ is the kinetic theory velocity.

A trial solution may be set up of the form:

$$\psi = \sum_{i=1}^{\infty} g_i(r^*)e^{-\phi_i z^*} \qquad (2)$$

where $r^* = r/r_o$ and $z^* = z/r_o$. For large ϕ_i, equation (2) may be expressed in terms of Bessel functions as follows:

$$\psi = \sum_{i=1}^{\infty} \frac{2\psi_o \, J_1[(\phi_i^2-B^2)^{1/2} r^*] \, e^{-\phi_i z^*}}{(\phi_i^2-B^2)^{1/2} \, J_1[(\phi_i^2-B^2)^{1/2}](1+\delta^2\phi_i^2)} \qquad (3)$$

A G. E. 235 digital computer was used to calculate values of ψ via equation (3) for the following values of the parameters:

$R = 0.5$ cm

$U = 500$ cm/sec

$D = 60$ cm^2/sec

$\psi_o = 0.002$

$\bar{w} = 6.28 \times 10^4$ cm/sec

$k_v = 9.25 \times 10^{-3}$ sec^{-1}

$\gamma = 0.554;\ 0.1;\ 0.05;\ 0.01$

The results are plotted in Figures 1A through 4A. For each γ value, graphs of ψ vs. r^* are given for a series of values of z^*. For our experimental conditions of a 0.1 cm long graphite cylinder in a tube of radius 0.5 cm, the graphite sample would extend from $z^* = 0$ to $z^* = 0.2$. It is clear that radial concentration gradients become increasingly severe with increasing values of γ.

The computer calculations are probably more useful for demonstration of general trends than in the analysis of experimental data. The calculations themselves are not free from approximations and they correspond to an idealized situation which is not likely to be realized in practice. The calculations were done for the case of $\phi_i >> \frac{2Ur_o}{D}$ and because of the nature of the equations, any possible dependence of the results on U is neglected. The completely general case cannot be conveniently solved in terms of Bessel functions, and even with the aid of a high speed digital computer, the computations are very laborious.

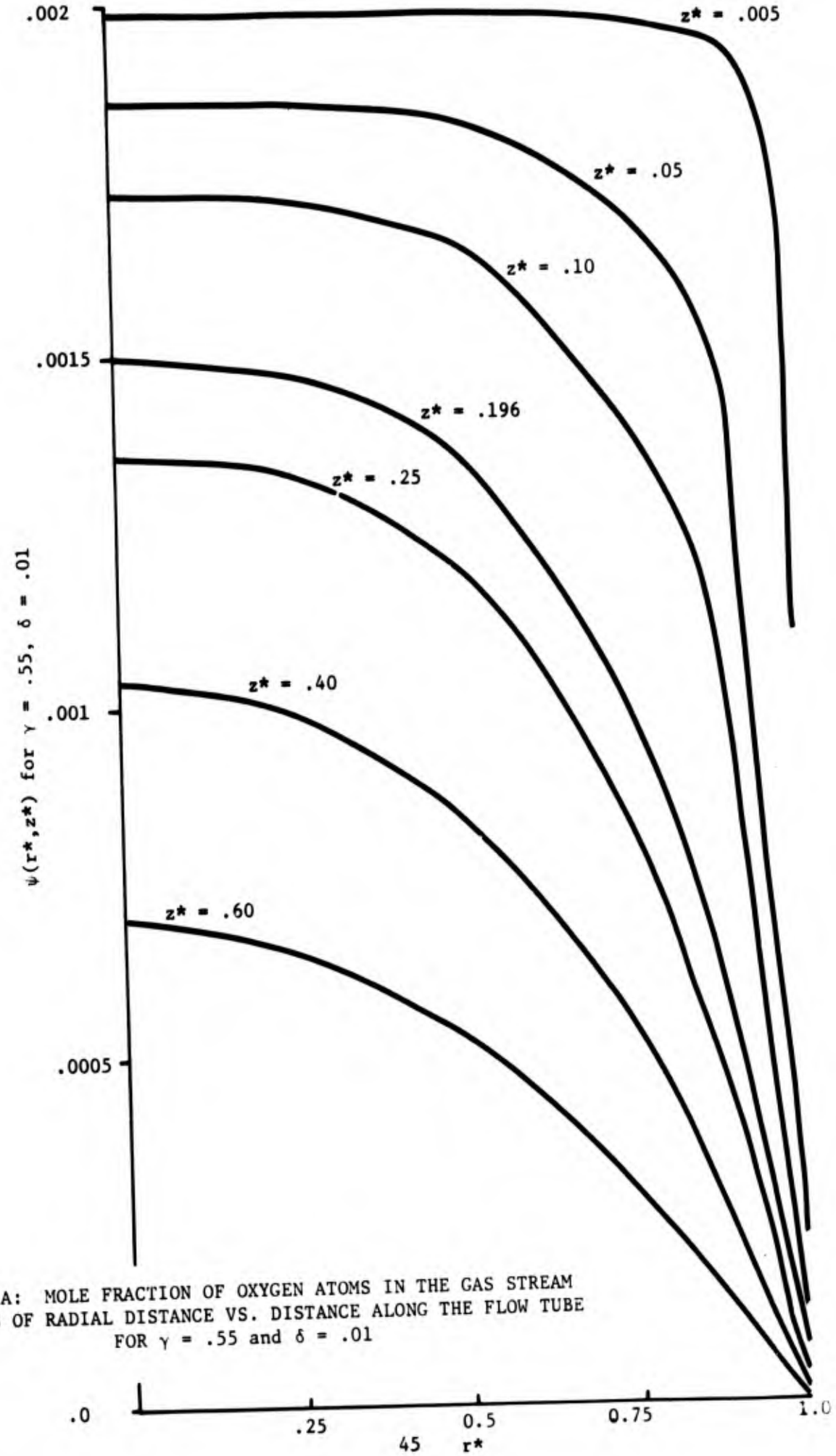

FIGURE 1A: MOLE FRACTION OF OXYGEN ATOMS IN THE GAS STREAM IN TERMS OF RADIAL DISTANCE VS. DISTANCE ALONG THE FLOW TUBE FOR $\gamma = .55$ and $\delta = .01$

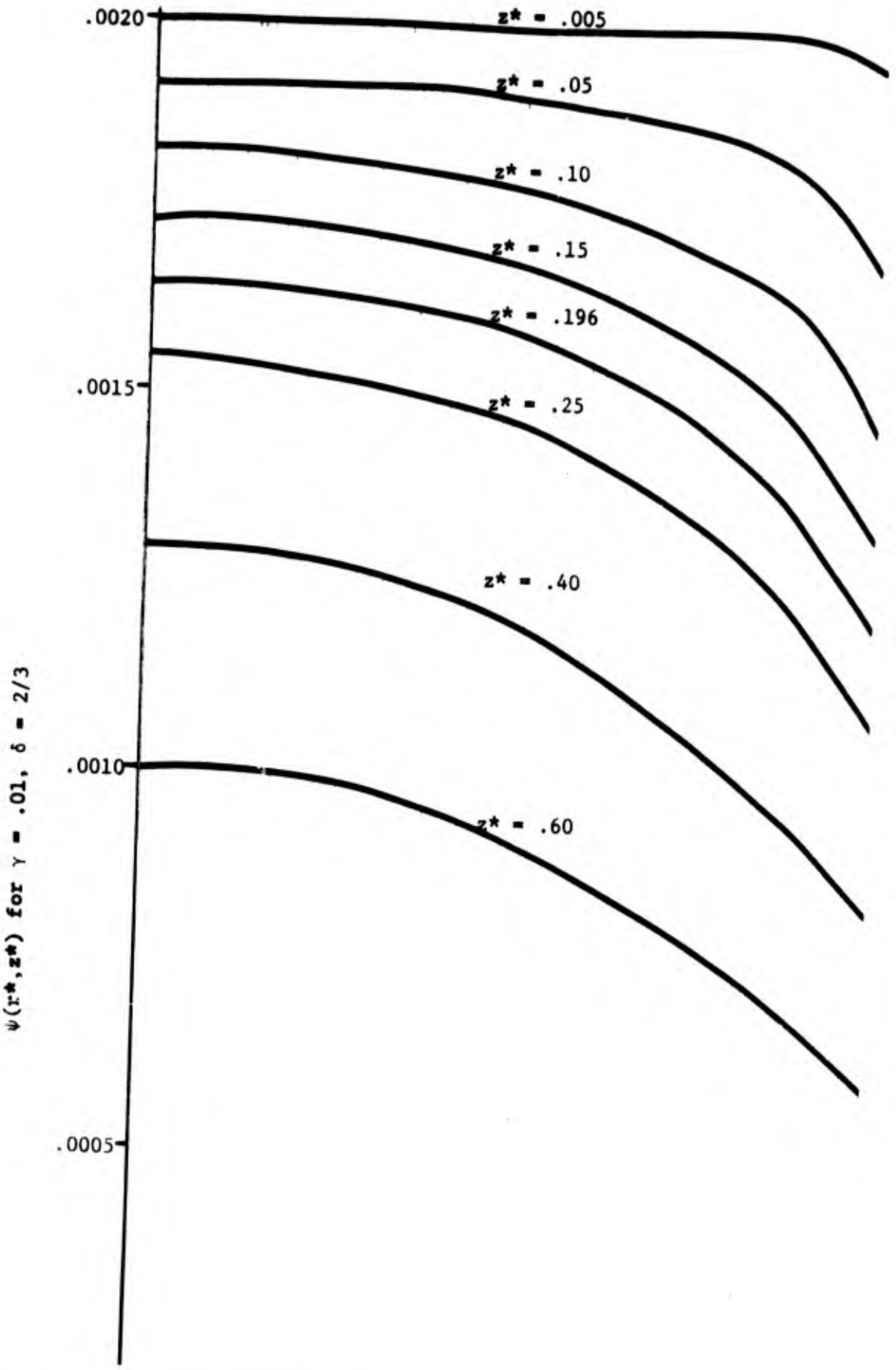

FIGURE 2A: MOLE FRACTION OF OXYGEN ATOMS IN THE GAS STREAM IN TERMS OF RADIAL DISTANCE VS. DISTANCE ALONG THE FLOW TUBE FOR $\gamma = .01$ and $\delta = 2/3$

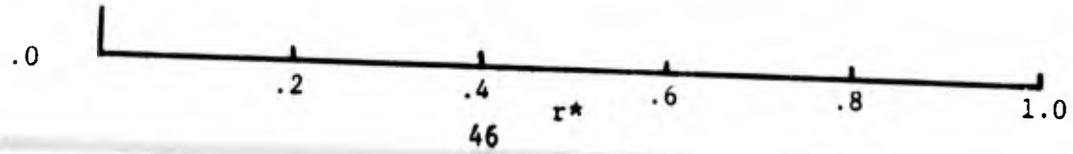

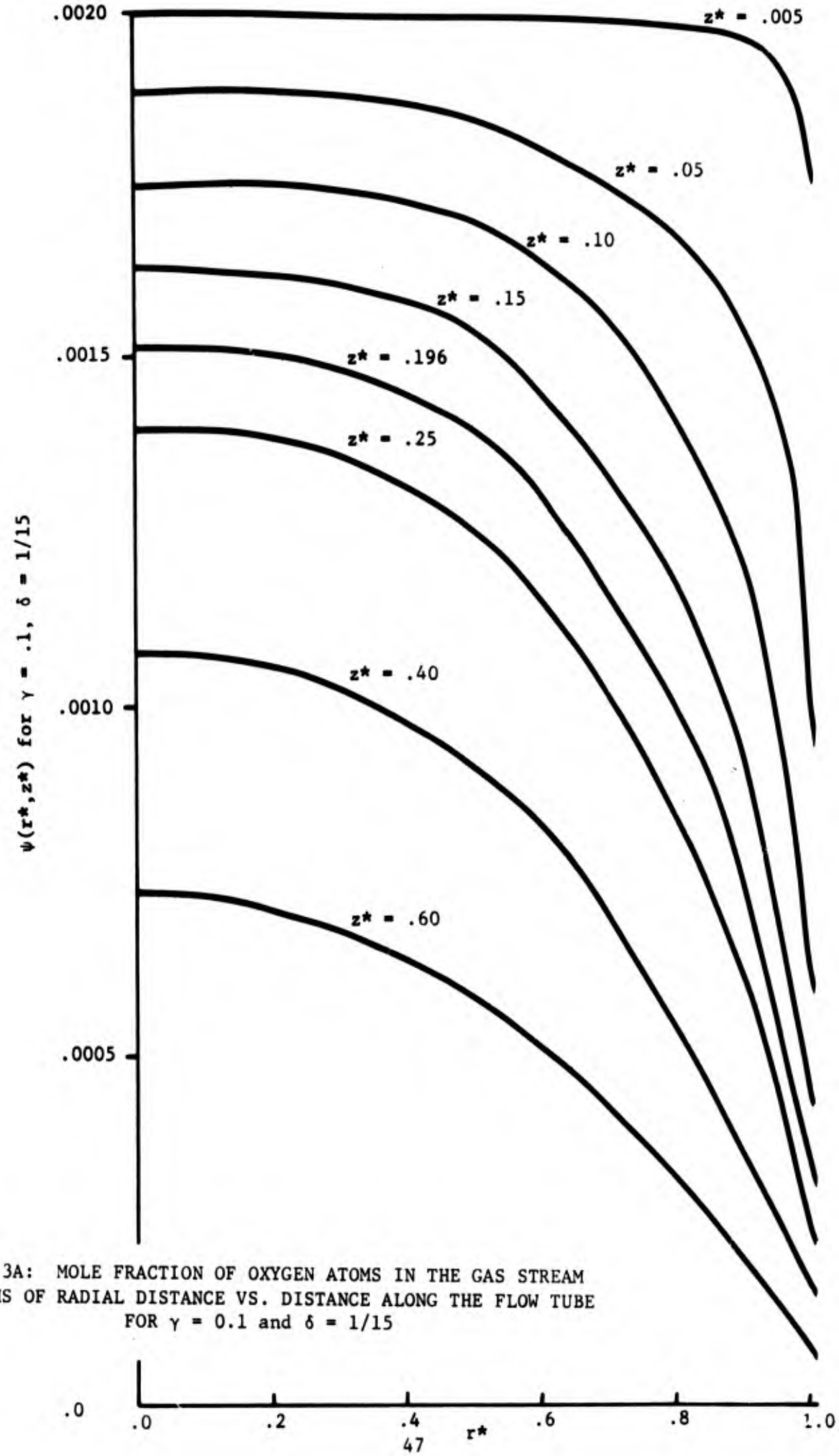

FIGURE 3A: MOLE FRACTION OF OXYGEN ATOMS IN THE GAS STREAM IN TERMS OF RADIAL DISTANCE VS. DISTANCE ALONG THE FLOW TUBE FOR $\gamma = 0.1$ and $\delta = 1/15$

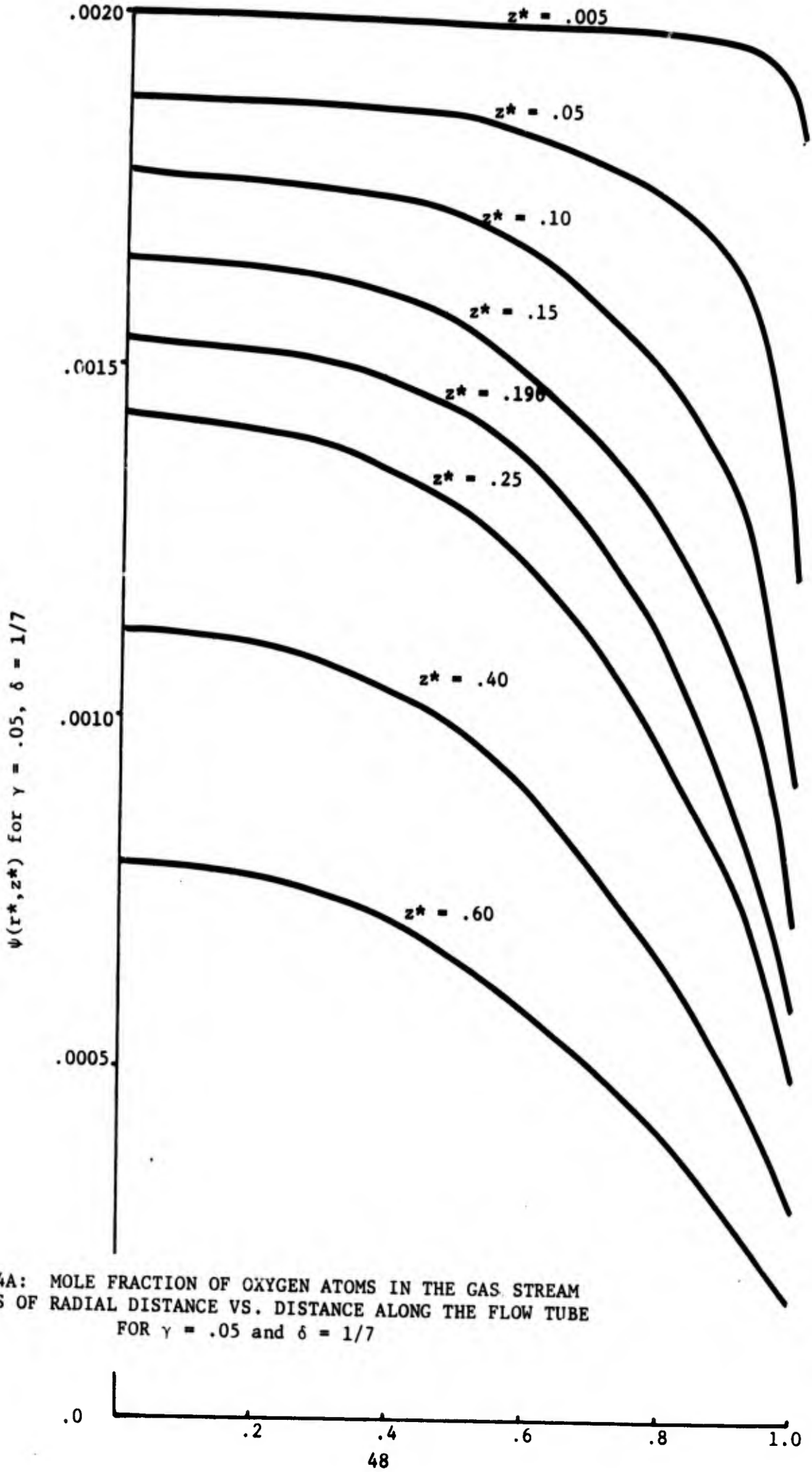

FIGURE 4A: MOLE FRACTION OF OXYGEN ATOMS IN THE GAS STREAM IN TERMS OF RADIAL DISTANCE VS. DISTANCE ALONG THE FLOW TUBE FOR $\gamma = .05$ and $\delta = 1/7$

REFERENCES

1. F. Kaufman, "Progress in Reaction Kinetics, Vol. 1," Pergamon Press (1961).

2. J. W. Linnett and D. G. H. Marsden, Proc. Roy. Soc., A234, 489, 504 (1956).

3. J. Nagle and R. F. Strickland-Constable, Proceedings of the Fifth Carbon Conference, Vol. 1, p. 154, Pergamon Press, Oxford (1962); also J. R. Walls and R. F. Strickland-Constable, Carbon 1, 333 (1964).

4. D. E. Rosner and H. D. Allendorf, AIAA J. 6, 650 (1968).

5. T. K. Sherwood, "Chemical Engineering Series--Adsorption and Extraction," McGraw-Hill (1937).

6. R. E. Walker, Physics of Fluids 4, 1211 (1961).

7. D. E. Rosner, AIAA J. 2, 593 (1964).

8. O. A. Hougen and K. M. Watson, "Kinetics and Catalysis," Part Three, John Wiley, N. Y. (1947).

9. JANAF Thermochemical Data

10. J. A. Fay, et. al., Aeronautical Sciences J., 25, No. 2, (1958).

11. J. W. Baughn and J. E. Arnold, Instrument Society of America, Los Angeles, October 4-7, 1965, Preprint No. 17, Dec. 2, 1965.

12. W. H. Carden, AIAA J., 27, Nov. 11, 1965.

13. W. H. Carden, DDC, Defense Supply Agency, July, 1965, AD466-165.

UNCLASSIFIED
Security Classification

DOCUMENT CONTROL DATA - R & D

(Security classification of title, body of abstract and indexing annotation must be entered when the overall report is classified)

1. ORIGINATING ACTIVITY (Corporate author)	2a. REPORT SECURITY CLASSIFICATION
Arthur D. Little, Incorporated 15 Acorn Park, Cambridge, Massachusetts	Unclassified
	2b. GROUP

3. REPORT TITLE

RESEARCH TO DETERMINE THE EFFECTS OF SURFACE CATALYCITY ON MATERIALS BEHAVIOR IN DISSOCIATED GAS STREAMS-ATJ-GRAPHITE

4. DESCRIPTIVE NOTES (Type of report and inclusive dates)

Final Report, for period 15 October 1968 to 31 January 1970

5. AUTHOR(S) (First name, middle initial, last name)

Joan B. Berkowitz-Mattuck

6. REPORT DATE	7a. TOTAL NO. OF PAGES	7b. NO. OF REFS
February 28, 1970	58	13

8a. CONTRACT OR GRANT NO.	9a. ORIGINATOR'S REPORT NUMBER(S)
F33615-69-C-1079 ✓ b. PROJECT NO. 7360 c. Task No. 736001 d.	9b. OTHER REPORT NO(S) (Any other numbers that may be assigned this report) AFML-TR-70-172

10. DISTRIBUTION STATEMENT This document is subject to special export controls and each transmittal to foreign governments or foreign nationals may be made only with prior approval of the Air Force Materials Laboratory (AFML/LPT), Wright-Patterson Air Force Base, Ohio 45433.

11. SUPPLEMENTARY NOTES	12. SPONSORING MILITARY ACTIVITY
None	Air Force Materials Laboratory Air Force Systems Command Wright-Patterson Air Force Base

13. ABSTRACT

The reactions of partially dissociated oxygen with heated ATJ graphite surfaces have been investigated at temperatures of 1600-2800°K and oxygen atom partial pressures of 7.0×10^{-3} to 7.4×10^{-2} torr. Measurements of total oxygen atom decay as a result of both chemical reaction and catalytic recombination were carried out by the $NO-NO_2$ light intensity method in a fast flow system. Weight change measurements were made to separate the total atom loss results into its two components. Mass spectrometric experiments were carried out over the temperature range 400-1200°K to determine product distribution as a function of oxygen molecule dissociation. The rate of net atom loss was found to be linear with time at a given partial pressure, and approximately first order in pressure. The net atom loss rate shows a maximum in the temperature interval investigated, the maximum shifting to higher temperatures with decreasing oxygen atom pressure. At an oxygen atom pressure of 3×10^{-5} atm, chemical reaction accounts for about 50% of the atom loss at low temperature, more than 60% of the atom loss in the neighborhood of maximum rate, and less than 35% of the atom loss at the highest temperatures investigated.

DD FORM 1 NOV 65 1473

UNCLASSIFIED
Security Classification

14 KEY WORDS	LINK A		LINK B		LINK C	
	ROLE	WT	ROLE	WT	ROLE	WT
Atomic Oxygen						
Graphite						
Heterogeneous Atom Recombination						
Oxidation						